THEORY AND OPERATION OF A CARBON DIOXIDE REDUCTION UNIT WITH SABATIER REACTION

By

Lenwood G. Clark

Thesis submitted to the Graduate Faculty of the

Virginia Polytechnic Institute

in candidacy for the degree of

MASTER OF SCIENCE

in

Engineering Mechanics

May 1968

THEORY AND OPERATION OF A CARBON DIOXIDE REDUCTION UNIT WITH SABATIER REACTION

by

Lenwood G. Clark

Thesis submitted to the Graduate Faculty of the

Virginia Polytechnic Institute

in partial fulfillment for the degree of

MASTER OF SCIENCE

in

Engineering Mechanics

APPROVED:

R. Thomas Davis
Chairman, Associate Professor

Associate Professor

Head, Engineering
Mechanics Department

Assistant Professor

May 1968

Blacksburg, Virginia

THEORY AND OPERATION OF A CARBON DIOXIDE REDUCTION UNIT WITH SABATIER REACTION

By

Lenwood G. Clark

ABSTRACT

A carbon dioxide reduction unit was studied in which carbon dioxide and hydrogen are reacted via the Sabatier reaction to produce methane and water. The unit is part of the oxygen recovery subsystem of an Integrated Life Support System (ILSS) at NASA's Langley Research Center. The study included an experimental investigation of the effects of feed-gas composition and flow rate, temperature, and pressure on reaction efficiency. Consideration is also given to the chemical equilibrium characteristics of the Sabatier reaction and an attempt is made to correlate experimental reactor performance with theory.

II. TABLE OF CONTENTS

III. ACKNOWLEDGMENTS

The author wishes to express his appreciation to the Langley Research Center of the National Aeronautics and Space Administration for its permission to use the material in this thesis.

In particular, the author wishes to express his gratitude to Mr. R. David Phillips for his assistance in conducting the experimental program and preparing thesis figures.

The author also thanks the staff of the Engineering Mechanics Department of the Virginia Polytechnic Institute for its guidance and criticism.

IV. LIST OF FIGURES AND TABLES

V. INTRODUCTION

Long duration space missions will ultimately require increased consideration and use of regenerative life support processes, including processes for oxygen recovery. A variety of candidate processes for accomplishing oxygen recovery are being developed through the cooperative efforts of governmental research laboratories and private industry. Many of these processes are surveyed and compared in references 1 to 4. In general, oxygen recovery requires two steps: first, removal of the metabolic carbon dioxide from the spacecraft's atmosphere and second, reduction of this carbon dioxide directly to oxygen or to water which is subsequently electrolyzed to produce oxygen. The end waste product of most of the physico-chemical processes which accomplish the reduction step is elemental carbon, which must be continuously removed from the process. Carbon removal problems, however, have been experienced with some of these processes, as noted in references 5 and 6, and represent a formidable obstacle to the development of reliable life support equipment. In addition, potential problems with carbon handling under conditions of reduced or zero gravity still remain to be solved.

One of the most promising carbon dioxide reduction processes is based on the "Sabatier" reaction, which does not produce elemental carbon. The reaction combines carbon dioxide (CO_2) and hydrogen (H_2) to produce methane (CH_4) and water (H_2O) according to the reaction:

$$CO_2 + 4H_2 \rightarrow 2H_2O + CH_4$$

Until 10 years ago, this reaction was chiefly considered for use in the production of gaseous fuel from coal. Recently, this reaction has been considered for use in oxygen recovery processes for space vehicles. As envisioned for this application, the product water from the Sabatier reaction and some makeup water would be electrolyzed to produce oxygen for crew consumption and hydrogen for the Sabatier reaction. Gas products from the Sabatier reaction, which would include some unreacted hydrogen and carbon dioxide, some uncondensed water, and mostly methane, would be vented to space. These losses constitute an important weight trade-off consideration and depend primarily on the reaction efficiency. The loss of carbon is not an important consideration since it comes from food, which would be stored as an expendable for a mission duration suitable for using the Sabatier process.

A variety of catalysts have been investigated, as reported in references 7 to 13, to determine which is most effective in promoting the Sabatier reaction to maximum water yield at minimum temperature conditions. Both pure metal powder and supported forms of Ruthenium and Nickel have been found to be effective catalysts with carbon dioxide conversion efficiencies of from 90 to 99 percent reported in the literature. Parameters such as temperature, feed-gas composition, pressure, reactor length-to-diameter ratio, and feed-gas flow rates have been found to affect conversion efficiencies. Several prototype oxygen recovery subsystems utilizing this reaction have also been developed and investigated to determine operating efficiencies and

component interactions. References 14 to 16 report the results of these investigations.

The present investigation was initiated to evaluate the performance of the Sabatier carbon dioxide reduction unit which is part of the Integrated Life Support System (ILSS) at NASA's Langley Research Center. The ILSS is a ground test prototype regenerative life support system designed to reclaim and reuse water and oxygen for a four-man crew while maintaining a comfortable atmosphere in a test chamber built to simulate a spacecraft cabin. A comprehensive summary of the 2-year development program is presented in reference 17 with recent test results discussed in references 5 and 6. This study was directed toward determining the optimum operating conditions for the ILSS Sabatier reactor, an unusual multitubed configuration which uses fluid cooling for temperature control. The study included an experimental investigation of the effects of feed-gas composition and flow rate, temperature, and pressure on reaction efficiency. In addition, consideration is also given to the chemical equilibrium characteristics of the Sabatier reaction and an attempt is made to correlate experimental reactor performance with theory.

VI. LIST OF SYMBOLS

a,b,c,d	stoichiometric coefficients
A,B	reactants
C,D	products of reaction
G	gas sample
G_T^o	standard Gibbs' free energy at temperature T, cal/g-mole
$\frac{(G_T^o - H_O^o)}{T}$	free-energy function, cal/g-mole
H_O^o	enthalpy of a compound or element at 0^o K, cal/g-mole
K	chemical equilibrium constant
M	molecular weight
P	theoretical reaction pressure, psia
P_{H_2O}	partial pressure of water vapor at the exhaust gas saturation temperature, psia
P_r	experimental reaction pressure, psia
R	universal gas constant, cal/(g-mole ^oK)
$\bar{R}$	volumetric feed-gas ratio, $H_2:CO_2$
S	space velocity, hr^{-1}
T	theoretical reaction temperature, ^oK
T_r	experimental reaction temperature, ^oF
T_s	exhaust gas saturation temperature, ^oF
V	Sabatier reactor core volume (excluding catalyst), ft^3
$\dot{W}$	weight flow rate of gas or liquid, lb/day
x	equilibrium mole fraction

x	volume fraction of exhaust gas constituents
X	number of moles of CO_2 at equilibrium
ΔG°	Gibbs' free-energy change in the standard state, cal/g-mole
$\Delta H^\circ_{f_0}$	standard heat of formation of 0° K, cal/g-mole
η_{CO_2}	carbon dioxide conversion efficiency, percent
ρ	density of gas, lb/ft^2

Subscripts

CH_4	methane
CO_2	carbon dioxide
H_2	hydrogen
H_2O	water
out	out of unit

VII. APPARATUS AND PROCEDURE

Test Apparatus

The experimental investigation was conducted in the NASA-Langley Integrated Life Support System (ILSS), which is shown in the photographs of figure 1. For this system, the oxygen recovery subsystem was designed in accordance with the materials balance shown in figure 2. Theoretically, it is possible to recover 7.48 lb/day of oxygen (four-man requirement at an average of 150-percent basal metabolism rate) from 56 percent of the available carbon dioxide and 4.21 lb/day of makeup water. A flow schematic of the Sabatier carbon dioxide reduction unit is shown in figure 3. For these tests H_2 and CO_2 were supplied from high purity gas bottles at regulated pressures of about 12 psig. Feed-gas pressures were further reduced to about 6 psig by low pressure regulators which ordinarily regulate the H_2 and CO_2 gas supply pressures from the ILSS H_2O electrolysis and CO_2 concentration units. Should the delivery pressure of either gas fall below 2.0 psig, solenoid valves close simultaneously as a safety feature. The desired flow rates of H_2 and CO_2 were obtained by adjusting individual flow valves according to the pressure drop across calibrated laminar flow elements. The mixed feed gas then passes through a desulfurization chamber which removes any sulfur or halides present, which could "poison" the Sabatier reaction catalyst by forming compounds on the catalyst surface, thereby decreasing the number of active reaction sites (refs. 8, 9, and 14). Although sulfur removal was not necessary for these tests, sulfur contamination

in the feed gas is possible from several sources within the ILSS. Minute quantities of sulfur generated by the crew could be present in the CO_2 delivered to the Sabatier reactor from the molecular sieve unit which concentrates metabolic CO_2 from the test chamber atmosphere. In addition, one of the H_2O electrolysis units under investigation uses an aqueous sulfuric acid (H_2SO_4) electrolyte. Carryover of this electrolyte through the liquid gas separation membranes into the hydrogen side of the electrolysis cells has been a problem as noted in references 5 and 6.

Conversion of the H_2 and CO_2 to H_2O and CH_4 occurs in the Sabatier reactor via the reaction:

$$CO_2 + 4H_2 \rightarrow 2H_2O + CH_4 + 1640 \frac{Btu}{lb} \text{ of } CO_2$$

Some of the exothermic heat of reaction is recovered when the hot exhaust products pass back through the desulfurization chamber to warm the feed gas. Reaction products as well as unreacted feed gas then pass through a condenser where product water is condensed. A porous plate H_2O separator is used to remove water from the unit under conditions of reduced or zero gravity. This component was not used, however, and the H_2O was collected in a trap to permit accurate measurement. Uncondensable exhaust products (small amounts of CO_2, H_2, and H_2O, and mostly CH_4) are vented through a back-pressure regulator to an external exhaust system (theoretically to space).

The desired reaction temperature is maintained by thermostatically circulating a silicon fluid (Dow Corning DC-331) at a temperature of

375° F through the Sabatier reactor. This fluid is supplied at a pressure of about 45 psig to the ILSS test chamber by a commercial heating and pumping unit and simulates a circuit for delivering waste heat to the life support system from a dynamic Brayton cycle radioisotope power system. When cooling is required the solenoid valve in the fluid circuit is de-energized and closed. The fluid, although at a temperature of 375° F, is supplied to the reactor as a coolant since reaction temperatures are much higher (400° to 700° F). The amount of fluid which flows through the reactor can be controlled with a manual valve to reduce reactor temperature fluctuations. In addition, an adjustable bleed orifice in the solenoid valve bypasses some of the fluid to reduce temperature fluctuations of another ILSS subsystem in series on the same fluid circuit. When the solenoid valve is closed the available fluid flow rate averages 70 lb/hr. When the solenoid valve opens, the fluid bypasses the reactor.

The condenser coolant was an aqueous solution of propylene glycol which was held at a nominal temperature of 32° F by a commercial cooling and pumping unit. This fluid circuit simulates the low temperature coolant fluid circuit which would be used as a heat-transfer loop in connection with a space radiator heat sink for temperature control. This fluid is supplied at 90 psig with a nominal flow rate of about 150 lb/hr to the condenser.

Sabatier reactor and catalyst description.- The Sabatier reactor is shown schematically in figure 4 and in the photographs of figure 5. The reactor is basically a cylinder with a length of 12.6 inches and a

diameter of 3.72 inches. It is constructed of ASME No. 316 stainless steel. Smaller in diameter near the bottom, the reactor is sealed with a metal conoseal and 3-inch-diameter Marmon flange clamp. Catalyst, in tablet form, is contained within the reactor between two perforated plates primarily in 12 tubes, which are 0.75 inch in diameter and about 9 inches long. The perforations in these plates permit gas flow through the catalyst bed, but are small enough (0.09 inch in diameter) to prevent migration of the catalyst.

The hot DC-331 fluid circulates in the chamber around the catalyst-filled tubes. The fluid enters the reactor near the bottom, flows upward from side to side around several diverter plates, and exits near the top. This fluid is also used for heating purposes while the reaction is being initiated. Once initiated, the reaction is exothermic and as previously mentioned, cooling is required if the desired reaction temperature is less than the passive equilibrium temperature. A sensing thermocouple (embedded 3.9 inches into one of the catalyst tubes) and optical meter relay control the fluid circuit solenoid valve. Should the temperature control mechanism fail, an auxiliary thermoswitch (embedded 5.5 inches into one of the catalyst tubes) closes the solenoid valve to initiate cooling when the reaction temperature reaches 650° F.

The 0.0287-cubic-foot volume of the reactor core is filled with 2.38 pounds (1081 grams) of promoted nickel catalyst. The catalyst is Harshaw N-0104 1/8-inch-diameter tablets which come fully activated and ready to use as supplied. It is composed of a catalyzing coating deposited on a carrier (physical support). The coating is a heterogeneous

mixture of about 58-percent nickel (Ni) and 42-percent nickel oxide (NiO) which represents 80 percent of the entire catalyst mass. The carrier, Kieselguhr (diatomaceous earth), comprises the remaining 20 percent of the catalyst mass. Although the specific process for preparing N-0104 is proprietary to The Harshaw Chemical Company, the general method used is to deposit a thin coating of nickel oxide on the Kieselguhr and then reduce the nickel oxide in a hydrogen atmosphere. The ratio of reduced nickel to total nickel for N-0104 is 0.60 to 0.65.

Desulfurization chamber and catalyst description.- The desulfurization chamber shown schematically in figure 6 and in the photographs of figure 5 is an assembly of concentric 3.0- and 3.5-inch-diameter cylindrical tubes constructed of ASME No. 316 stainless steel. The overall unit length is 11.7 inches with sealing at the bottom in the same manner as the Sabatier reactor. Desulfurization catalyst, in extrusion form, is contained in the inner tube between two perforated plates 9.5 inches apart. The hot product gases from the Sabatier reactor enter the annular passage between the two cylinders near the bottom, circulate around the inner tube, and exit near the top. The cool feed-gas mixture of CO_2 and H_2 flows through the desulfurization catalyst bed for sulfur removal and is warmed prior to entering the Sabatier reactor. Warming the feed gas acts to reduce the temperature gradient along the Sabatier reactor and to reduce the condenser cooling requirements. Both the Sabatier reactor and desulfurization chamber were insulated with several inches of fiberglass batting.

The 0.0371-cubic-foot volume of the desulfurization chamber core is filled with 2.84 pounds (1287 grams) of essentially pure zinc oxide. The catalyst is Harshaw Zn-0401 3/16-inch-long extrusions. This material does not actually perform as a true catalyst since in the sulfur removal process it gets converted to the corresponding anions of zinc.

Gas Analysis

The composition of the inlet and outlet gases to the Sabatier reactor was determined by passing samples into a Beckman, Model 320-D, process gas chromatograph. Gas analysis is subsequently accomplished by comparison of the thermal conductivity of the components of the sample gas to the thermal conductivity of a reference carrier gas. This chromatograph has four columns for separating the sample into its components. Two identical Carbowax[1] 20-M® columns are to strip out the higher molecular weight organic compounds and retard water vapor. Carbon dioxide is retained and eluted from a silica gel column which also retards water vapor. The last column, a molecular sieve, is used for separating hydrogen, oxygen (O_2), nitrogen (N_2), methane, and carbon monoxide (CO). Two samples are taken simultaneously for measurement: one 0.3 milliliter and the other 3.0 milliliters in size. The smaller sample is used for gases in high concentration (0 to 100 percent by volume) and was used for the majority of the measurements during these tests. The larger sample is used for the low concentration (0 to

[1]Union Carbide trade name.

5 percent by volume) gases. A complete analysis of all components in both samples required 20 minutes.

High purity helium (assayed 99.9997 percent by volume) was used for the carrier gas at a pressure of 20 psig at the instrument's metering orifice with a nominal flow rate of 36 cubic centimeters per minute. The thermal conductivity detector was operated at 100° C with a bridge voltage and current of 15 volts and 110 milliamperes, respectively. Instrument output was read on a Brown -0.1 to 1.0 millivolt recorder. With full-scale deflection equivalent to 100-percent volumetric concentration of the sample gas constituent, the accuracy of reading the recorder chart paper was within ±0.2 percent.

The chromatograph was calibrated frequently for all gases being analyzed. The primary calibration gas was a mixture: 20.2-percent CO_2, 21.1-percent H_2, 22.9-percent N_2, 18.6-percent CH_4, and 17.2-percent CO (by volume). Calibration gases of essentially pure CH_4 and H_2 were also used. The calibration curves for CO_2 and CH_4 (with thermal conductivities at 100° C of 5.06×10^{-5} and 9.99×10^{-5} cal/(sec-cm° C), respectively) are linear and accurate within ±1 percent. Hydrogen, however, with its high conductivity of 49.94×10^{-5} cal/(sec-cm° C) compared to the reference gas, helium, with conductivity of 39.85×10^{-5} cal/(sec-cm° C), causes poor instrument response. The calibration curve for H_2 is nonlinear and measurements were made with an accuracy of ±4 percent.

Instrumentation

The desired flow rates of H_2 and CO_2 were obtained by adjusting manual flow valves according to the pressure drop across calibrated

Meriam laminar flow elements. These flow elements were calibrated for the particular feed gas at regulated pressure with a Precision Scientific wet test meter which is accurate to within ±1 percent. The differential pressures for H_2 and CO_2 flows were measured with 0 to 5 and 0 to 10 inches of water Magnehelic pressure gages with 0.1 and 0.2 inch of water divisions, respectively. The reactor pressure was measured with a 0 to 5 psig Magnehelic pressure gage with 0.1 psi divisions.

Iron Constatan thermocouple probes were used for measuring temperature. The Sabatier reactor control temperature was read on a 0° to 750° F Sim-Ply-Trol pyrometer with 10° F divisions. The desulfurization chamber temperature (7.5 inches into the catalyst bed) and the Sabatier reactor temperature (5.9 inches into the catalyst bed) were read on a 75° to 2300° F thermoelectric pyrometer with 50° F divisions. The exhaust gas saturation temperature was read on a 0° to 350° F Honeywell pyrometer with 5° F divisions.

Test Procedure

To verify its integrity prior to testing, the Sabatier CO_2 reduction unit was pressurized with gaseous N_2 and the leakage rate was determined for ambient temperature. This was accomplished by measuring the pressure decay rate of a known makeup supply volume while the unit pressure was maintained constant at 10 psig. The total unit leakage rate for these conditions was subsequently found to be less than 3 cc/min.

Warmup.- Warmup of the Sabatier reactor was accomplished by circulating hot DC-331 through the reactor while maintaining a slow

CO_2 flow to purge the system of contaminants. When the reaction control temperature reached 330° F, the H_2 flow rate was set for about 1.5 lb/day and the CO_2 flow rate was adjusted to the corresponding stoichiometric value. When the temperature increased to about 350° F, indicating reaction initiation, the fluid flow control valve was closed. The temperature was then allowed to increase until the desired value was reached at which time thermostatic cooling was initiated. Reactor warmup to a temperature of 500° F was generally accomplished in 1 hour. The selected H_2 flow rate was then set by adjusting the appropriate valve. An arbitrary CO_2 flow rate was similarly obtained. The desired reaction pressure was obtained by adjusting the exhaust gas back-pressure regulator. As soon as the reactor control temperature had stabilized, test data were obtained.

Data run.- For a stabilized test condition the inlet CO_2 concentration was measured with the gas chromatograph. Assuming the remainder of the feed gas to be H_2, the H_2:CO_2 volumetric feed-gas ratio was then calculated to within ±1 percent since the CO_2 measurement was that accurate. The water trap was then drained to a reference mark on the sight glass and product water was collected for some time period, usually 1 hour. During this period the composition of the uncondensable gas products being exhausted was measured. Two gas chromatograph readings (20 minutes apart) were taken for this purpose and the readings averaged. Near the end of the test time period, the inlet feed-gas ratio was again determined to insure that test conditions had not altered. Data runs where either the inlet or the outlet readings varied significantly

were disregarded. At the conclusion of the data run the product water was drained and measured with a graduated cylinder. The CO_2 flow rate was then varied and the above procedure repeated until tests for the selected condition were completed.

Data analysis.- The CO_2 conversion efficiency, η_{CO_2}, for a given data run can be determined from the expression

$$\eta_{CO_2} = \left[\frac{\dot{W}_{CO_2} - \left(\dot{W}_{CO_2}\right)_{out}}{\dot{W}_{CO_2}}\right] \times 100 \tag{1}$$

where $\dot{W}_{CO_2}$ and $\left(\dot{W}_{CO_2}\right)_{out}$ are the flow rates of CO_2 entering and leaving the system, respectively. The flow rate of the CO_2 feed gas entering is

$$\dot{W}_{CO_2} = \frac{\rho_{CO_2}\dot{W}_{H_2}}{\rho_{H_2}\bar{R}} \tag{2}$$

where $\bar{R}$ is the volumetric feed-gas ratio, $H_2{:}CO_2$, and ρ_{CO_2}, ρ_{H_2} are the densities of CO_2 and H_2, respectively, at ambient conditions. The flow rate of the CO_2 in the exhaust gas can be calculated from the expression

$$\left(\dot{W}_{CO_2}\right)_{out} = \frac{x_{CO_2}M_{CO_2}\left(\dot{W}_{H_2} + \dot{W}_{CO_2} - \dot{W}_{H_2O}\right)}{x_{CO_2}M_{CO_2} + x_{H_2}M_{H_2} + x_{CH_4}M_{CH_4} + x_{H_2O}M_{H_2O}} \tag{3}$$

where $\left(\dot{W}_{H_2} + \dot{W}_{CO_2} - \dot{W}_{H_2O}\right)$ is the total flow rate of the exhaust gas leaving the system; M_{CO_2}, M_{H_2}, M_{CH_4}, M_{H_2O} are the molecular weights of the exhaust gas constituents; and x_{CO_2}, x_{H_2}, x_{CH_4}, x_{H_2O} are the volume fractions of the exhaust gas constituents. The composition of the exhaust gas was determined by the gas chromatograph with the exception of the water constituent. The concentration of water can be calculated from

$$x_{H_2O} = \frac{P_{H_2O}}{(P_r - 0.3)} \tag{4}$$

where P_{H_2O} is the partial pressure of the water vapor at the exhaust gas saturation temperature, T_s, and $(P_r - 0.3)$ is the approximate total pressure at the system exhaust.

Another useful design parameter is the space velocity, S, the inverse of which is a measure of the dwell time of the reactant gases in the reactor core. Space velocity is defined as the hourly volume flow of feed gas at standard conditions[1] per unit volume of the reactor core (excluding the catalyst) and is given by

$$S = \frac{1}{24V}\left(\frac{\dot{W}_{H_2}}{\rho_{H_2}} + \frac{\dot{W}_{CO_2}}{\rho_{CO_2}}\right) \tag{5}$$

Previous investigators (refs. 7 and 8) have found that high space velocities, in excess of 500 to 600 per hour, result in reduced CO_2

[1]Standard conditions will be taken as 70° F, 14.7 psia which is the same as the assumed ambient conditions.

conversion efficiency. Space velocities ranging from 174 to 765 per hour were investigated during this study.

Sample data analysis.- To illustrate the use of the above analysis procedure, data recorded during run No. 22 are analyzed. The following data were recorded: $T_r = 500^\circ$ F, $P_r = 16$ psia, $\dot{W}_{H_2} = 1.0 \frac{lb}{day}$, $\dot{W}_{H_2O} = 4.24 \frac{lb}{day}$, $\overline{R} = 3.67$, $T_s = 73^\circ$ F, $x_{CO_2} = 0.101$, $x_{H_2} = 0.046$, and $x_{CH_4} = 0.812$. The densities of H_2 and CO_2 at 70° F and 14.7 psia are 0.0052 and 0.1144 lb/ft^3, respectively.

The flow rate of CO_2 entering the system for these conditions is

$$\dot{W}_{CO_2} = \frac{0.1144(1.0)}{0.0052(3.67)} = 5.99 \frac{lb}{day}$$

The partial pressure of the water vapor leaving the system at the saturation temperature of 73° F is 0.4019 psia from reference 18. The volume fraction of the water constituent is then

$$x_{H_2O} = \frac{0.4019}{(16 - 0.3)} = 0.026$$

The flow rate of CO_2 leaving the system is, therefore,

$$\left(\dot{W}_{CO_2}\right)_{out} = \frac{0.101(44.01)(1.0 + 5.99 - 4.24)}{0.101(44.01) + 0.046(2.016) + 0.812(16.04) + 0.026(18.02)}$$

$$\left(\dot{W}_{CO_2}\right)_{out} = 0.681 \frac{lb}{day}$$

The CO_2 conversion efficiency for this data run is then calculated to be

$$\eta_{CO_2} = \left(\frac{5.99 - 0.681}{5.99}\right) \times 100 = 88.6$$

which means that of the 5.99 lb/day of CO_2 entering the system, 88.6 percent was converted to CH_4 and H_2O.

The volume of the reactor core is 0.0287 cubic feet and the space velocity for this condition is

$$S = \frac{1}{24(0.0287)}\left(\frac{1.0}{0.0052} + \frac{5.99}{0.1144}\right) = 355 \text{ hr}^{-1}$$

and the dwell time is about 10 seconds.

VIII. ANALYSIS

Chemical equilibrium exists when the rates of forward and reverse reactions are equal (ref. 19). Thus, for a typical reaction $aA + bB \rightleftarrows cC + dD$, there exists an equilibrium constant, K, defined by

$$K = \left[\frac{x_C^c x_D^d}{x_A^a x_B^b}\right] P^{c+d-a-b} \tag{1}$$

where P is the reaction total pressure, x is the equilibrium mole fraction, A and B are the reactants, C and D are the products, and a, b, c, and d are the stoichiometric coefficients.

For the Sabatier reaction $CO_2 + 4H_2 \rightarrow CH_4 + 2H_2O$, the equilibrium relation is

$$K = \frac{x_{CH_4}\left(x_{H_2O}\right)^2}{x_{CO_2}\left(x_{H_2}\right)^4 P^2} \tag{2}$$

Following the example of reference 8, if the degree of conversion of CO_2 is represented by X, then the number of moles of CO_2 at equilibrium is $1 - X$, of H_2 is $4 - 4X$, of CH_4 is X, of H_2O is $2X$, and the total present is $5 - 2X$.

For the stoichiometric $H_2:CO_2$ ratio of 4:1, the equilibrium relation becomes

$$K = \frac{X(2X)^2(5 - 2X)^5}{(1 - X)(4 - 4X)^4(5 - 2X)^3P^2} = \frac{X^3(5 - 2X)^2}{64(1 - X)^5P^2} \qquad (3)$$

For the 2.5-percent hydrogen rich condition having a $H_2:CO_2$ ratio of 4.1:1, for example, the equilibrium relation becomes

$$K = \frac{X(2X)^2(5.1 - 2X)^2}{(1 - X)(4.1 - 4X)^4P^2} \qquad (4)$$

From the Gibbs' free-energy relationship enthalpies and standard heats of formation, the equilibrium constants may be calculated as a function of temperature. This calculation is given in Appendix A for reaction temperature from 200° to 800° F and figure 7 shows the result.

The effects of various parameters on the maximum possible CO_2 conversion may be determined by relating the mole fraction of CO_2 at equilibrium directly to reaction temperature. This can be accomplished by calculating the value of the equilibrium constant from the governing equation for the selected $H_2:CO_2$ ratio for values of equilibrium CO_2 mole fraction and reaction pressure. The corresponding reaction temperature can then be interpreted from figure 7.

Figure 8 was subsequently calculated and shows the maximum possible CO_2 conversion at several pressures as a function of reaction temperature for a stoichiometric $H_2:CO_2$ ratio of 4:1. It can be seen that it is desirable to operate the reaction at as low a temperature as possible for essentially complete conversion. Low temperature reactions, however, are difficult to initiate and sustain. In addition, at low temperatures,

condensation of the product water in the reactor could have the undesirable effect of decreasing the effectiveness of the catalyst (ref. 8). Ideally, it would be desirable to operate the reactor isothermally at 300° F with the inlet gases heated to this temperature. In practice, however, there is usually a temperature gradient in the reactor bed, with the inlet temperature running higher than the outlet temperature because of the exothermic heat release. Conversion would subsequently be lower at the reactor inlet and as reactor bed temperature decreased at the outlet, conversion would increase.

Figure 8 also shows that an increase in reaction pressure causes a corresponding increase in CO_2 conversion. The effect of pressure becomes negligible at temperatures where essentially complete conversion is achieved.

An increase in CO_2 conversion is possible for operation with a H_2:CO_2 ratio greater than 4.0, which would correspond to a hydrogen rich condition, as shown in figure 9. However, this effect becomes diminished as the amount of excess hydrogen increases as shown in figure 10.

IX. RESULTS AND DISCUSSION

The results of experimental studies of the effects of various parameters on the CO_2 conversion efficiency of the Sabatier reaction are presented in tables 1 and 2. These tables list the various data and calculations for 98 of a total 130 data runs, which were made during this study. Those data missing were either deleted because of inaccuracy or to avoid duplication. Table 1 presents data for 72 data runs at a reaction pressure of 16 psia. At this pressure, tests were primarily conducted for H_2 flow rates of 1.0, 1.5, and 2.0 lb/day with reaction temperatures of 400°, 500°, and 600° F. The H_2:CO_2 feed-gas ratio varied from 2.7 to 5.25. No adjustment of gas chromatograph data was made. The average total percentage of outlet gas constituents was 100.46 percent with the standard deviation being ±1.51 percent, which was well within instrument accuracy. Table 2 presents data for 26 data runs conducted at a reaction pressure of 20 psia. At this pressure, the H_2 flow rate was maintained constant at 1.0 lb/day with reaction temperatures of 400°, 500°, and 600° F. The H_2:CO_2 feed-gas ratio varied from 2.45 to 4.87. The average total percentage of outlet gas constituents was 100.94 percent with the standard deviation being ±1.62 percent, which was again within instrument accuracy.

Inspection of the tabulated data shows that occasionally up to 15 percent more water is produced than is theoretically possible. It is unlikely that this error can be attributed to mistakes in either gas analyses, water and time period measurements, or laminar flow element calibration. The source of the error was not determined, however, most

likely the H_2 differential pressure gage was misread and the flow rate incorrectly set. If the H_2 flow rate were 15 percent higher than anticipated, the calculated CO_2 conversion efficiency would be high by 5 percent.

The data listed in tables 1 and 2 are presented graphically in figures 11 and 12. Some of the data have been replotted in figures 13 to 15 to better illustrate the effects of selected parameters on CO_2 conversion efficiency.

Effect of Excess Hydrogen

The effect of excess H_2 (above stoichiometric requirements) on CO_2 conversion efficiency is shown in figures 11 and 12. As predicted by theory (fig. 10), conversion efficiency can be seen to vary directly with the amount of excess H_2 for a constant reaction temperature, with the effect becoming diminished as the amount of excess H_2 increases. It should be noted that for these figures a small variation in the total quantity of gas which passes through the reactor occurs with varying excess H_2 flow for otherwise constant conditions. Such a small change in space velocity, as noted later, does not affect subsequent interpretation.

For a H_2 flow rate of 1.0 lb/day, which is the approximate design condition, a conversion efficiency approaching 98 percent is possible at 600° F for stoichiometric feed conditions at both test pressures as shown in figures 11(a) and 12. Conversion efficiency increases slightly to about 99 percent for a 3-percent hydrogen-rich feed condition.

At lower reaction temperatures, as noted later, the conversion efficiency is lower with an increased amount of excess H_2 required to achieve essentially complete conversion.

If an amount of excess H_2 were available it could be used in one of two ways: Either to operate the reactor with hydrogen-rich feed and improve conversion efficiency, or to operate the reactor with stoichiometric feed and reduce an additional amount of the available excess CO_2 (shown in fig. 2) which would otherwise be vented to space. Obviously, the choice lies with the method which produces the largest yield of water. The data of figures 11 and 12 tend to indicate that hydrogen-rich feed operation of this reactor is not justified. The data of figure 11(a) for a reaction temperature of 500° F can be used to illustrate this trade-off as follows:

$H_2:CO_2$	$\dot{W}_{H_2}$ (lb/day)	$\dot{W}_{CO_2}$ (lb/day)	η_{CO_2} (percent)	$\dot{W}_{H_2O}$ (lb/day)
4.0	1.0	5.50	95	4.28
4.4	1.1	5.50	99	4.46
4.0	1.1	6.05	95	4.70

If 0.1 pound of excess H_2 were available and used to operate the reactor with a 10 percent hydrogen-rich feed, 4.46 pounds of water would result. However, if this H_2 were used to reduce an additional amount of CO_2, 4.70 pounds of water would result, or 0.24 pounds more than produced by the other method. However, if all of the H_2 were reacted, 4.50 and 4.95 pounds of water would result, respectively. It is apparent that complete H_2 conversion, and not complete CO_2 conversion, would

result in the largest yield of water, since H_2 is available in a limited quantity. The available excess CO_2 should therefore be used to operate the reactor carbon dioxide-rich to eliminate any unreacted H_2 from being vented to space.

Effect of Pressure

The effect of reaction pressure on CO_2 conversion efficiency may be determined by comparing figure 11(a) with figure 12. This comparison is shown in figure 13 for a H_2 flow rate of 1.0 lb/day. Increasing the reaction pressure from 16 to 20 psia causes a corresponding increase in conversion efficiency with effect becoming diminished as essentially complete conversion is achieved. It can be seen that the effect of pressure on conversion efficiency agrees with theoretical predictions (fig. 8); however, the trend with temperature cannot be correlated, as noted later. The effect of pressure is most noticeable in figure 13(a) for a reaction temperature of 400° F where for stoichiometric feed conditions, conversion efficiency is increased from 91 to 96 percent. At 600° F, however, the effect of pressure is negligible with conversion efficiency approaching 98 percent for stoichiometric feed conditions. At this temperature the reaction pressure could be selected to be consistent with the pressure requirements of the other units which form the ILSS oxygen recovery subsystem.

Effect of Temperature

The effect of reaction temperature on CO_2 conversion efficiency is shown in figure 14. Figures 11(a), 11(c), and 12 also show this effect, but less clearly. Comparing figure 14 with figure 9 shows that the

effect of temperature with all other factors remaining equal was generally as predicted. Chemical equilibrium theory indicates that essentially conversion is possible up to a given temperature, and that conversion will decrease if all of the reactor bed were above this temperature. Figure 14 shows that increasing the reaction temperature beyond about 600° F causes a decrease in conversion efficiency. Operation at a higher temperature could produce undesirable product of reaction; namely, carbon monoxide and carbon as noted in reference 9. It should be noted that the theory is based on an isothermal situation which exists only to a limited degree with the present reactor configuration and makes precise temperature correlation difficult. A temperature gradient existed along the length of the catalyst bed and the reaction temperature, T_r, served only as a reference measurement. A second thermocouple (embedded 5.9 inches into one of the catalyst tubes or 2 inches deeper than the control thermocouple) consistently indicated up to 100° F lower temperature.

Effect of Flow Rate

The effect of feed-gas flow rate (expressed as space velocity) on CO_2 conversion efficiency is shown in figure 15 for a selected set of constant conditions. For space velocities of less than about 600 per hour, which would be equivalent to reactor dwell times of greater than 6 seconds, the effect of flow rate appears negligible. At higher space velocities, however, a gradual decrease in conversion efficiency results. This is in good agreement with the results of previous investigations (refs. 7 and 9).

Additional Observations

Several chemical analyses of the product water from the Sabatier carbon dioxide reduction unit were made. These analyses showed that the water contained up to 45 parts per million (by weight) of nickel ions which undoubtedly is the result of the nickel catalyst. Direct disassociation of this water in an electrolysis unit to complete the oxygen recovery process could present problems over a long period of time. If the electrolysis unit used an acid electrolyte, the nickel ions could plate out on the hydrogen electrode. If a basic electrolyte were used, the nickel ions could form a flocculant. The effect of contamination such as this in the water being processed in an electrolysis unit warrants further investigation. The requirement of processing this water in a water recovery subsystem for contaminant removal may be necessary prior to electrolysis.

The ILSS Sabatier carbon dioxide reduction unit was operated for a period of 336 hours during this investigation. During this period the thermostatically controlled fluid circuit which was used for reactor temperature control functioned exceedingly well. This temperature control feature enabled reaction temperatures to be changed as desired during the investigation. However, once optimum operating conditions have been determined, a Sabatier reactor could be designed to operate at those conditions without the need for such a sophisticated temperature control.

X. CONCLUDING REMARKS

An experimental investigation has been made of the effects of various parameters on the performance of a Sabatier carbon dioxide reduction unit which is part of an Integrated Life Support System. A brief attempt at correlating experimental reactor performance with theory was also made. The study suggests the following conclusions:

1. The Sabatier carbon dioxide reduction unit was operated for 336 hours during which time the unit demonstrated the capability of operating reliably over a range of feed-gas compositions and flow rates, temperatures, and pressures. When the unit was operated with stoichiometric feed, carbon dioxide conversion efficiencies from about 91 to 98 percent were achieved for "indicated" reaction temperatures from 400° to 600° F, respectively.

2. At all temperatures tested, operation with an excess amount of hydrogen feed (above stoichiometric requirements) improved conversion efficiency. However, hydrogen-rich operation of a Sabatier reactor as part of an oxygen recovery subsystem would not be justified since complete conversion of the available H_2 would result in the largest yield of water. A larger yield of oxygen would subsequently result when the water was electrolyzed.

3. At the optimum operating temperature, 600° F, the effect on conversion efficiency of changing reactor pressure from 16 to 20 psia was negligible. At lower temperatures where conversion was less complete, conversion efficiency was higher at the higher pressure.

4. The effect of space velocity on conversion efficiency was found to be insignificant at space velocities of less than 600 per hour, which would be equivalent to reactant gas dwell times in the reactor of greater than 6 seconds.

5. The effects of reaction temperature, pressure, and feed-gas composition on carbon dioxide conversion efficiency were found to be generally as predicted by chemical equilibrium theory. Since the reactor was non-isothermal, however, precise correlation of experimental reactor performance with theory was not possible.

XI. REFERENCES

1. Dole, S. H.; Tamlin, A. R.: The Sabatier Reaction for Inorganic Recovery of Oxygen in Manned Space Capsules. RM-2542 (Contract No. AF 49(368)-700), The Rand Corporation, February 25, 1960.

2. Bialecki, Adolph: Comparative Feasibility and Logistics of Oxygen Recovery Systems. Presented at the Seventh Annual Meeting of the American Astronautical Society, Dallas, Texas, January 16-18, 1961. Preprint (61-16).

3. Hendel, Frank J.: Gaseous Environment During Space Missions. Journal of Spacecraft and Rockets, vol. 1, no. 4, July-August 1964.

4. Macklin, Martin: Carbon Dioxide Reduction Systems. Presented at the AIAA Fourth Manned Space Flight Meeting, St. Louis, Missouri, October 11-13, 1965.

5. Hypes, Warren D.: Life Support Systems Integration. Presented at the Conference on Bioastronautics, Virginia Polytechnic Institute, August 14-18, 1967.

6. Pecoraro, J. N.; Pearson, A. O.; Drake, G. L.; and Burnett, J. R.: Contributions of a Developmental Integrated Life Support System to Aerospace Technology. Presented at the AIAA Fourth Annual Meeting and Technical Display, Anaheim, California, October 23-27, 1967.

7. Rydelek, R. F.: Investigation of Integrated Carbon Dioxide Hydrogeneration Systems. ASD-TDR 64-581 (Contract No. AF 33(616)8323), AiResearch Manufacturing Company, A Division of the Garrett Corporation, October 1962.

8. Remus, G. A.; Ferris, R. W.; and Zeff, J. D.: Catalytic Reduction of Carbon Dioxide to Methane and Water. GATC Final Report MRD 1249-2030 (Contract No. AF 33(615)1210), MRD Division, General American Transportation Corporation, December 1964.

9. Thompson, Edward B., Jr.: Investigation of Catalytic Reactions for CO_2 Reduction, Part I. Evaluation of a Nickel-Keiselguhr Catalyst. FDL-TDR 64-22, Part I, Air Force Flight Dynamics Laboratory, October 1964.

10. Thompson, Edward B., Jr.: Investigation of Catalytic Reactions for CO_2 Reduction, Part II. Evaluation of Base Metal Oxide Catalysts. FDL-TDR 64-22, Part II, Air Force Flight Dynamics Laboratory, April 1965.

11. Thompson, Edward B., Jr.: Investigation of Catalytic Reactions for CO_2 Reduction, Part III. Evaluation of Precious Metal Catalysts. FDL-TDR 64-22, Part III, Air Force Flight Dynamics Laboratory, October 1965.

12. Thompson, Edward B., Jr.: Investigation of Catalytic Reactions for CO_2 Reduction, Part IV. Experimental Analysis of Catalyst-Reactor Configuration Combinations. FDL-TDR 64-22, Part IV, Air Force Flight Dynamics Laboratory, February 1966.

13. Ames, Robert K.: Sabatier Reactor Performance Using Ruthenium and Nickel Catalyst at Sea Level and Reduced Pressure. Presented at the Fourth Space and Flight Equipment Symposium, San Diego, California, October 4-7, 1966.

14. Ames, Robert K.: Development of the Sabatier Life Support System. Presented at the Institute of Environmental Sciences Annual Technical Meeting, Chicago, Illinois, April 11-13, 1962.

15. Ames, Robert K.: Present Status of the Sabatier Life Support System. Presented at the Aviation and Space, Hydraulic, and Gas Turbine Conference and Products Show, Los Angeles, California, March 3-7, 1963. ASME Paper 63-AHGT-48.

16. Smith, J. M.; Olcott, T. M.: Independent Development in Advanced Life Support Systems. LMSC-672047, Lockheed Missiles and Space Company, December 1966.

17. Armstrong, R. C.: Life Support System for Space Flights of Extended Time Periods. NASA CR-614 (Contract No. NAS1-2934), Convair Division of General Dynamics, November 1966.

18. Keenan, Joseph H.; and Keyes, Frederick G.: Thermodynamic Properties of Steam. First ed., John Wiley and Sons, Inc., 1948.

19. Lewis, Gilbert Newton; and Randall, Merle: Thermodynamics. Second ed., McGraw-Hill Book Co., Inc., 1961.

20. Shortley, George; and Williams, Dudley: Elements of Physics. Third ed., Prentice-Hall, Inc., 1961.

21. Rossini, Frederick D.; Wagman, Donald D.; Evans, William H.; Levine, Samuel; and Jaffe, Irving: Selected Values of Chemical Thermodynamic Properties. NBS Circular 500, National Bureau of Standards, February 1, 1952.

22. Rossini, Frederick D.; Pitzer, Kenneth S.; Taylor, William J.; Ebert, Joan P.; Kilpatrick, John E.; Beckett, Charles W.; Williams, Mary G.; and Werner, Helene G.: Selected Values of Properties of Hydrocarbons. NBS Circular C461, National Bureau of Standards, November 1947.

XII. VITA

The author was born in [redacted] on [redacted] He graduated from Hampton High School in Hampton, Virginia, in 1956. In September of that year he entered the Norfolk Division of William and Mary-Virginia Polytechnic Institute. He participated in the Cooperative Engineering Program and was employed by the National Advisory Committee for Aeronautics, Langley Field, Virginia. In June 1959, he transferred to the Virginia Polytechnic Institute in Blacksburg, Virginia, and received the degree of Bachelor of Science in Engineering Mechanics in June 1961. After graduation, he was employed by the Langley Research Center of the National Aeronautics and Space Administration. In June 1964, he returned to the Virginia Polytechnic Institute to begin studies toward the degree of Master of Science in Engineering Mechanics.

XIII. APPENDIX A

DERIVATION OF EQUILIBRIUM CONSTANT, K, FROM FREE-ENERGY AND ENTHALPY DATA

The equilibrium constant, K, is related to the Gibbs' free-energy change in the standard state, ΔG°, according to the formula:

$$-\frac{\Delta G^\circ}{T} = R \ln K$$

where T is the reaction temperature ($^\circ$K) and R the universal gas constant (1.9870 cal/g-mole $^\circ$K (ref. 20)). The quantity $\frac{\Delta G^\circ}{T}$ may be evaluated from

$$\frac{\Delta G^\circ}{T} = \sum \left(\frac{G_T^\circ - H_0^\circ}{T} + \frac{\Delta H_{f_0}^\circ}{T} \right)_{Prod} - \sum \left(\frac{G_T^\circ - H_0^\circ}{T} + \frac{\Delta H_{f_0}^\circ}{T} \right)_{React}$$

where

G_T° = standard Gibbs' free energy at temperature T

H_0° = enthalpy of the compound or element at 0° K

$\Delta H_{f_0}^\circ$ = standard heat of formation at 0° K

Table 3 lists the free-energy function, $\frac{(G_T^\circ - H_0^\circ)}{T}$, and the heat of formation, $\Delta H_{f_0}^\circ$, for the various elements and compounds of interest for several temperatures. The heat of formation data were obtained

from reference 21 and the free-energy function data by linear interpolation from reference 22.

Calculation of the equilibrium constant for the Sabatier reaction $CO_2 + 2H_2 \rightarrow 2H_2O + CH_4$ at 477° K (400° F) is as follows:

$$\frac{\Delta G^\circ}{T} = -40.305 - \frac{15990}{477} - 2\left(40.881 + \frac{57107}{477}\right) + 47.251 + \frac{93965}{477} + 4(27.596)$$

$$\frac{\Delta G^\circ}{T} = -40.305 - 33.522 - 321.204 + 47.251 + 196.991 + 110.384$$

$$\frac{\Delta G^\circ}{T} = -40.405 \ \frac{\text{cal}}{(\text{g-mole } ^\circ\text{K})}$$

$$ln\ K = -\frac{\Delta G^\circ}{RT} = \frac{40.405}{1.987} = 20.335$$

$$\log_{10} K = \frac{20.335}{2.303} = 8.829$$

Therefore, $K = 6.745 \times 10^8$ for 477° K (400° F).

Table 4 lists the Sabatier reaction equilibrium constants for reaction temperatures of 200° to 800° F. These constants were calculated in the manner indicated.

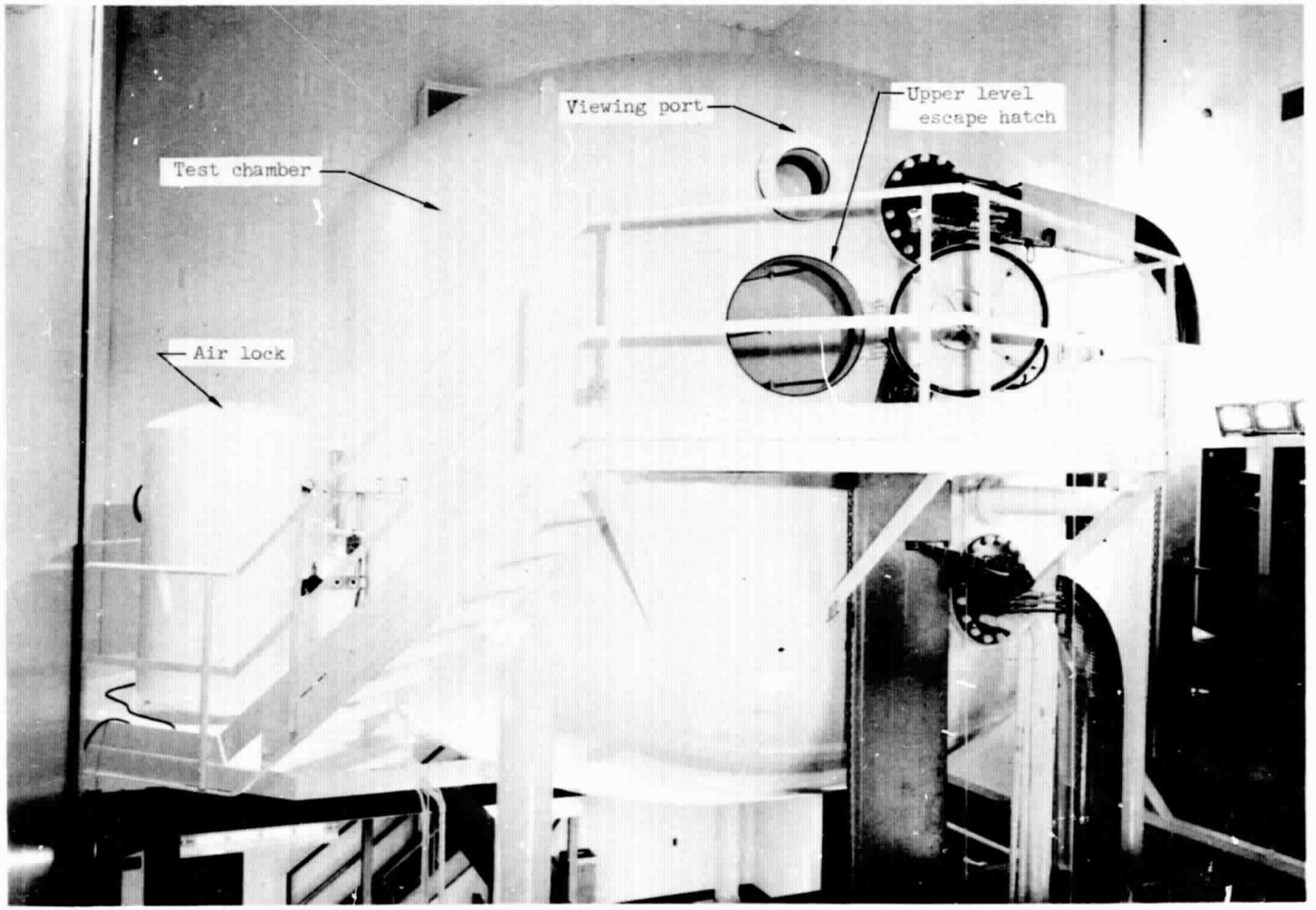

(a) Exterior view

Figure 1.- The NASA-Langley Integrated Life Support System (ILSS).

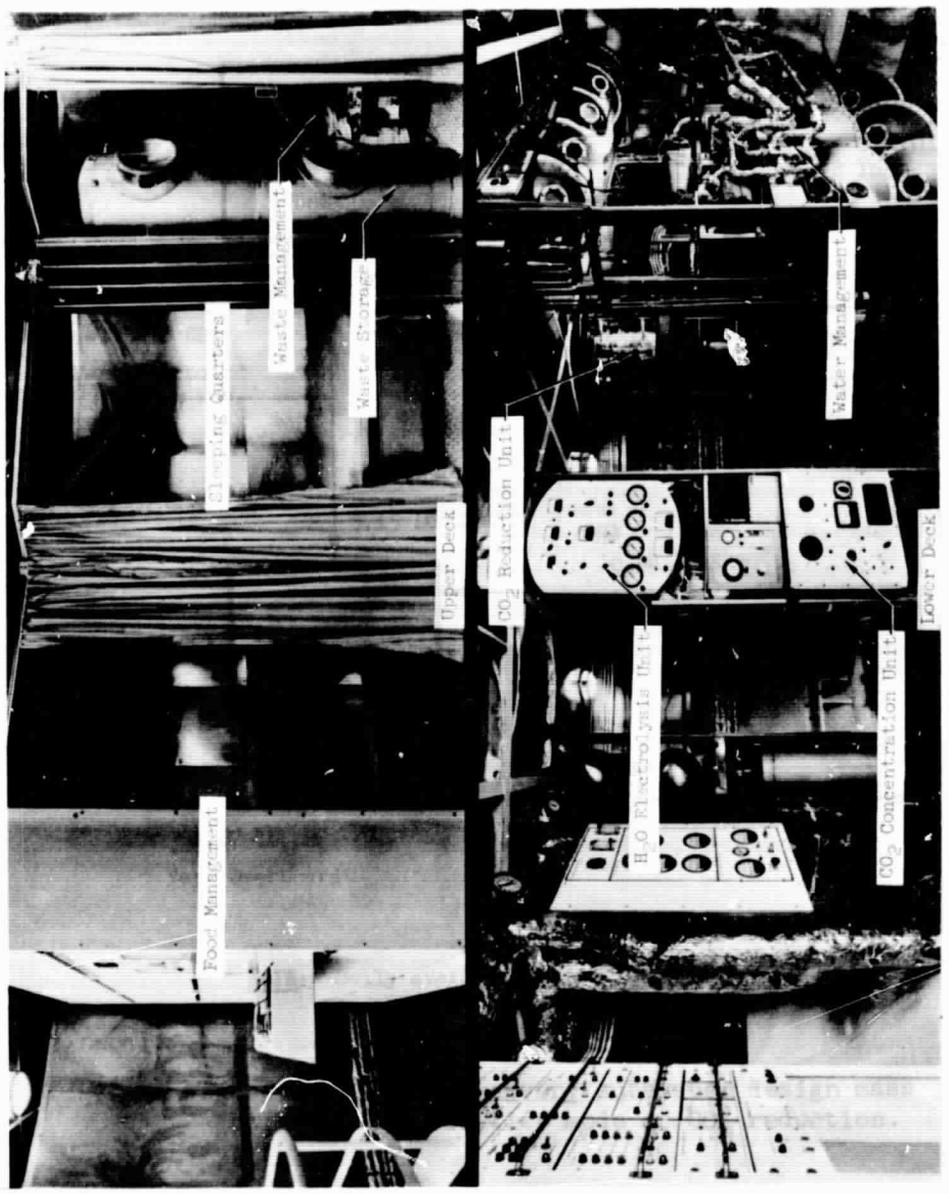

(b) Interior view

Figure 1.- Concluded.

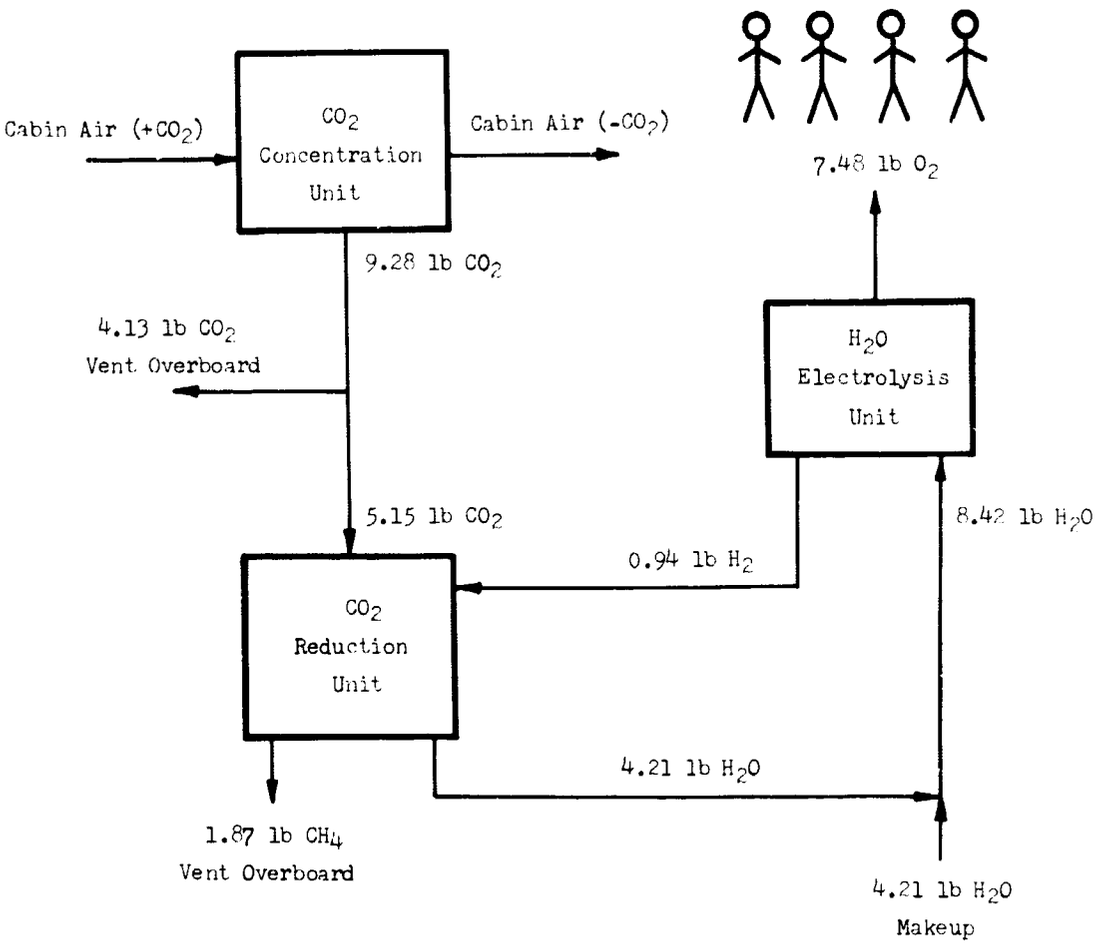

NOTE: Daily averages for four-man crew.

Figure 2.- Oxygen recovery subsystem design mass balance with Sabatier mode of CO_2 reduction.

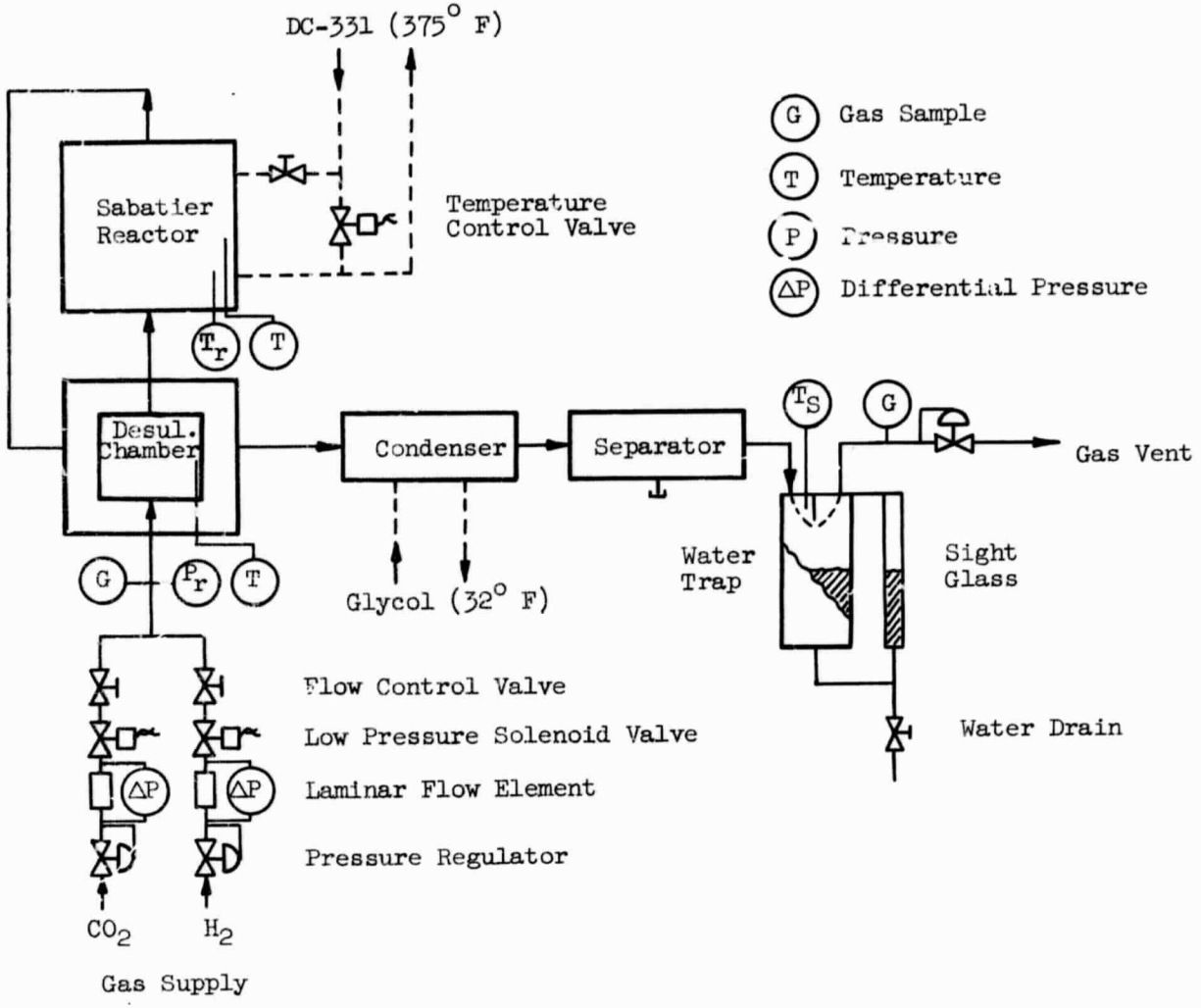

Figure 3.- Sabatier CO_2 reduction unit flow schematic.

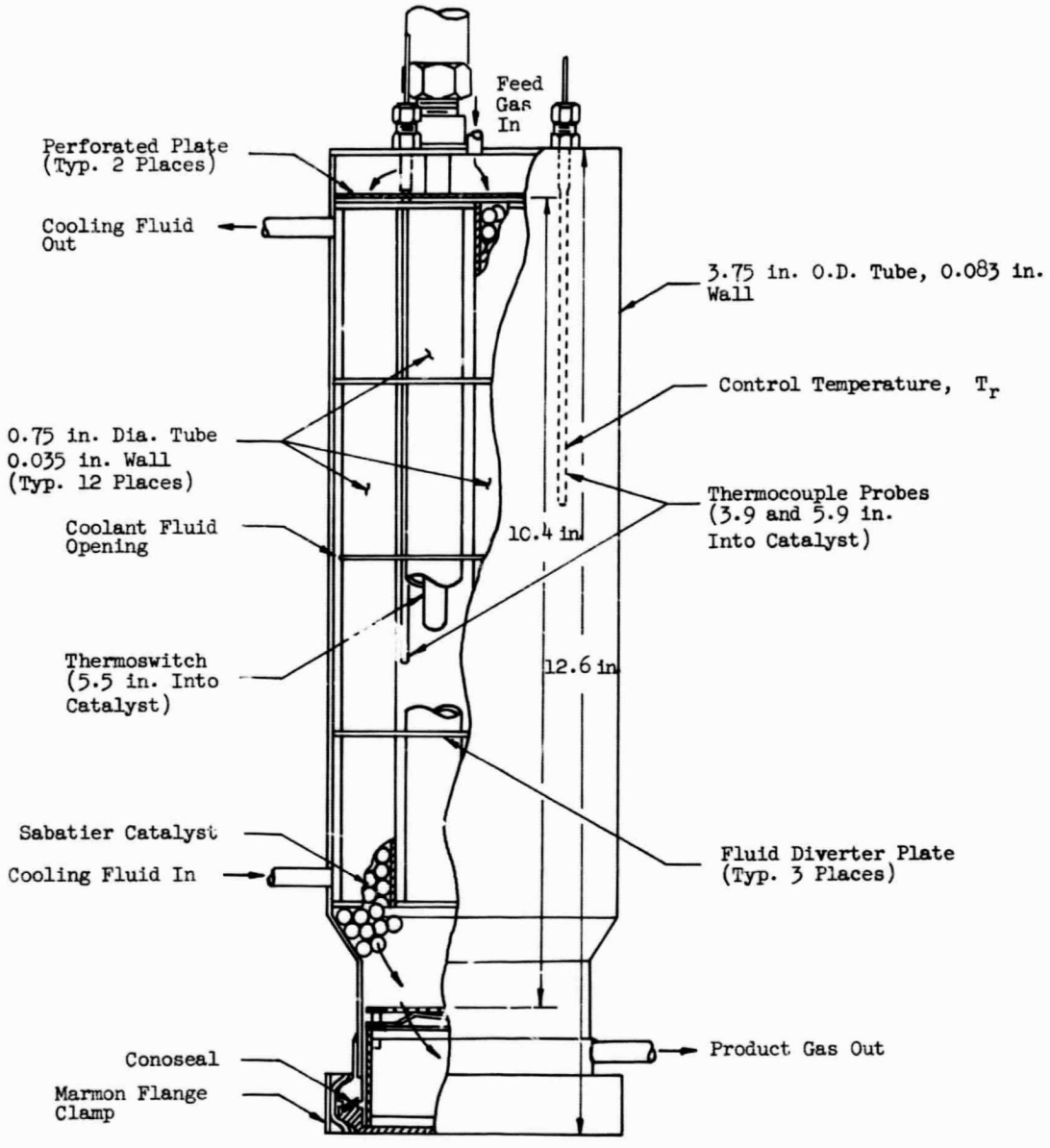

Figure 4.- Sabatier reactor schematic.

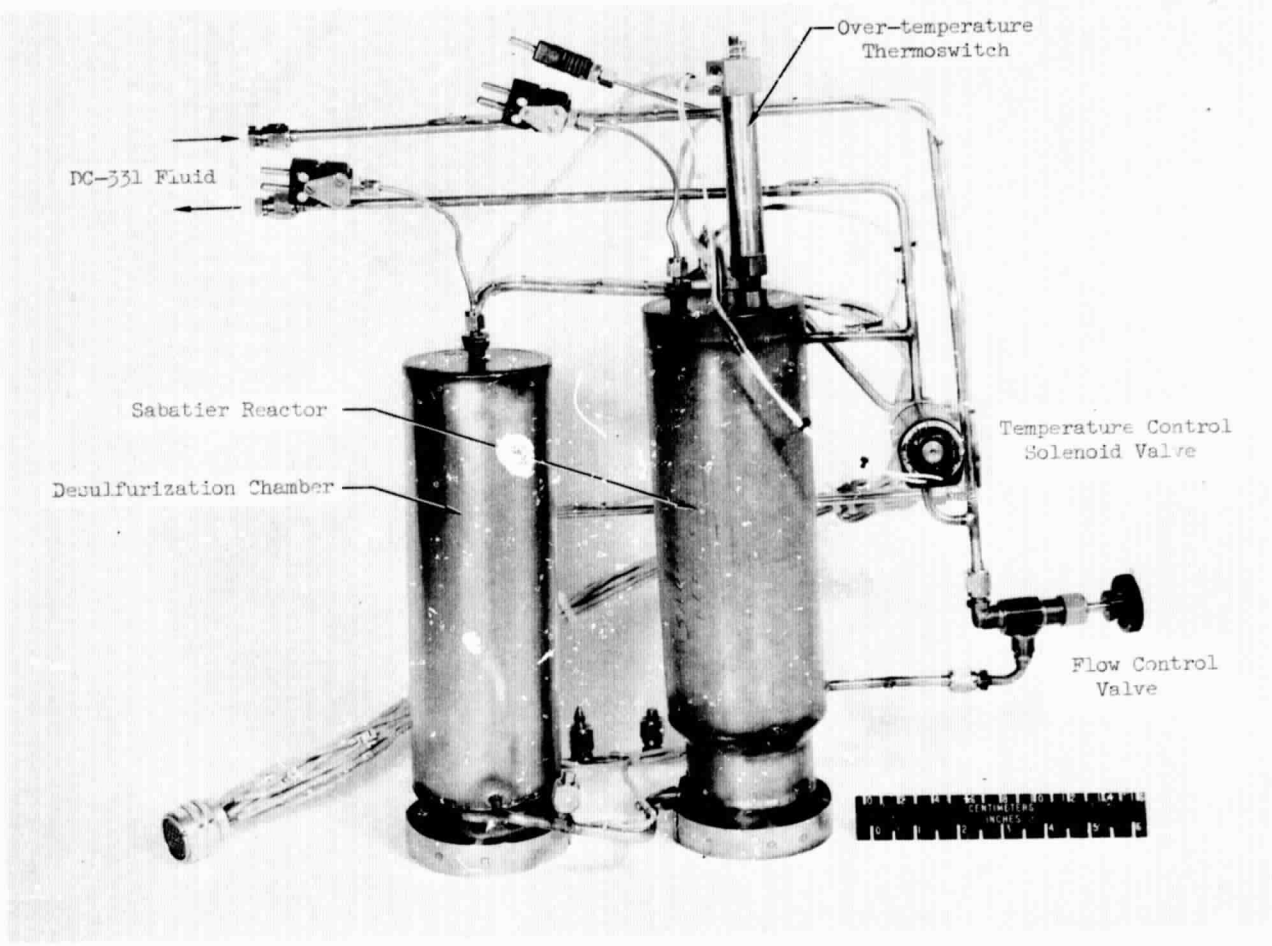

(a) View showing assembly

Figure 5.- Sabatier reactor and desulfurization chamber.

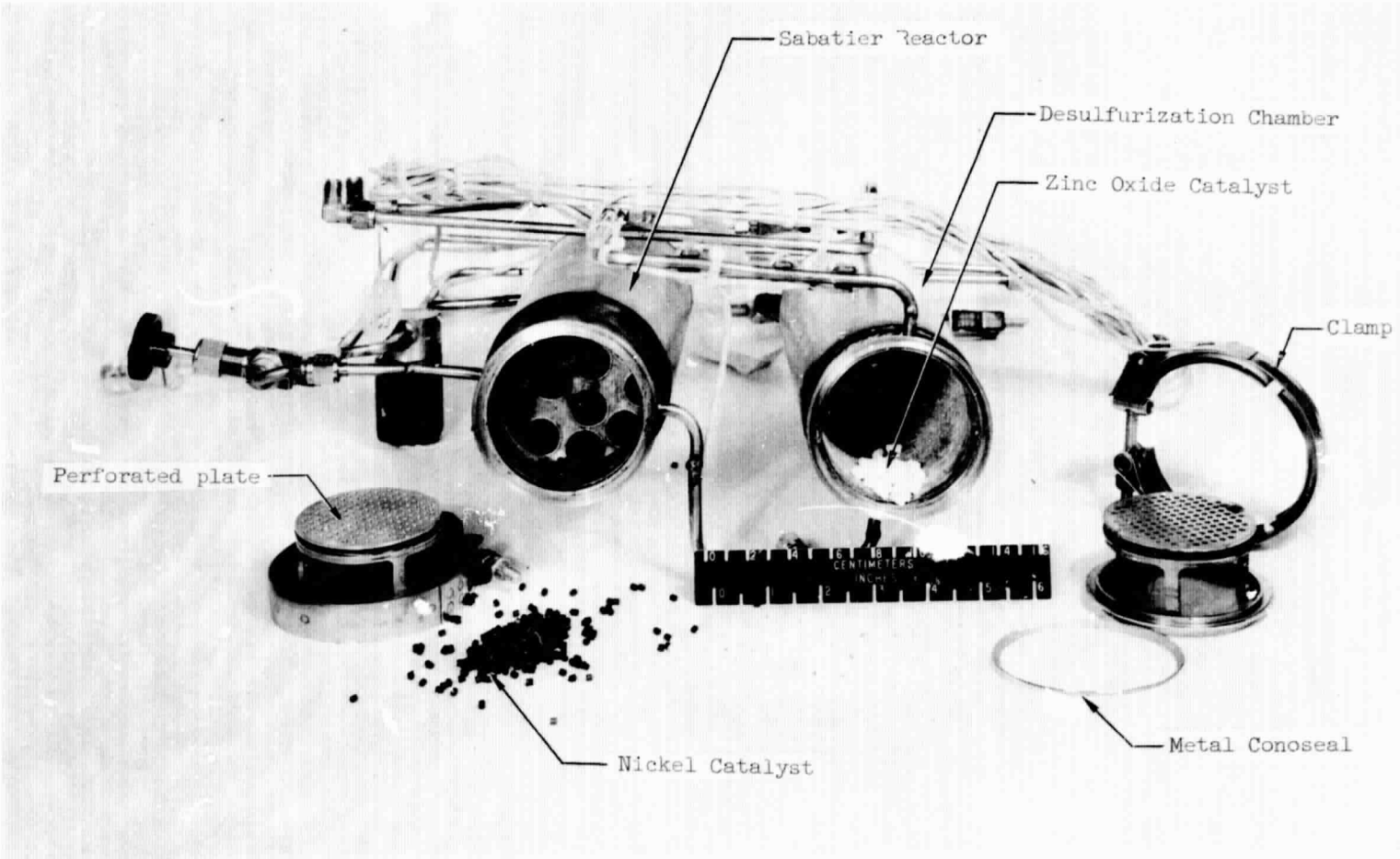

(b) View showing catalyst arrangement

Figure 5.- Concluded.

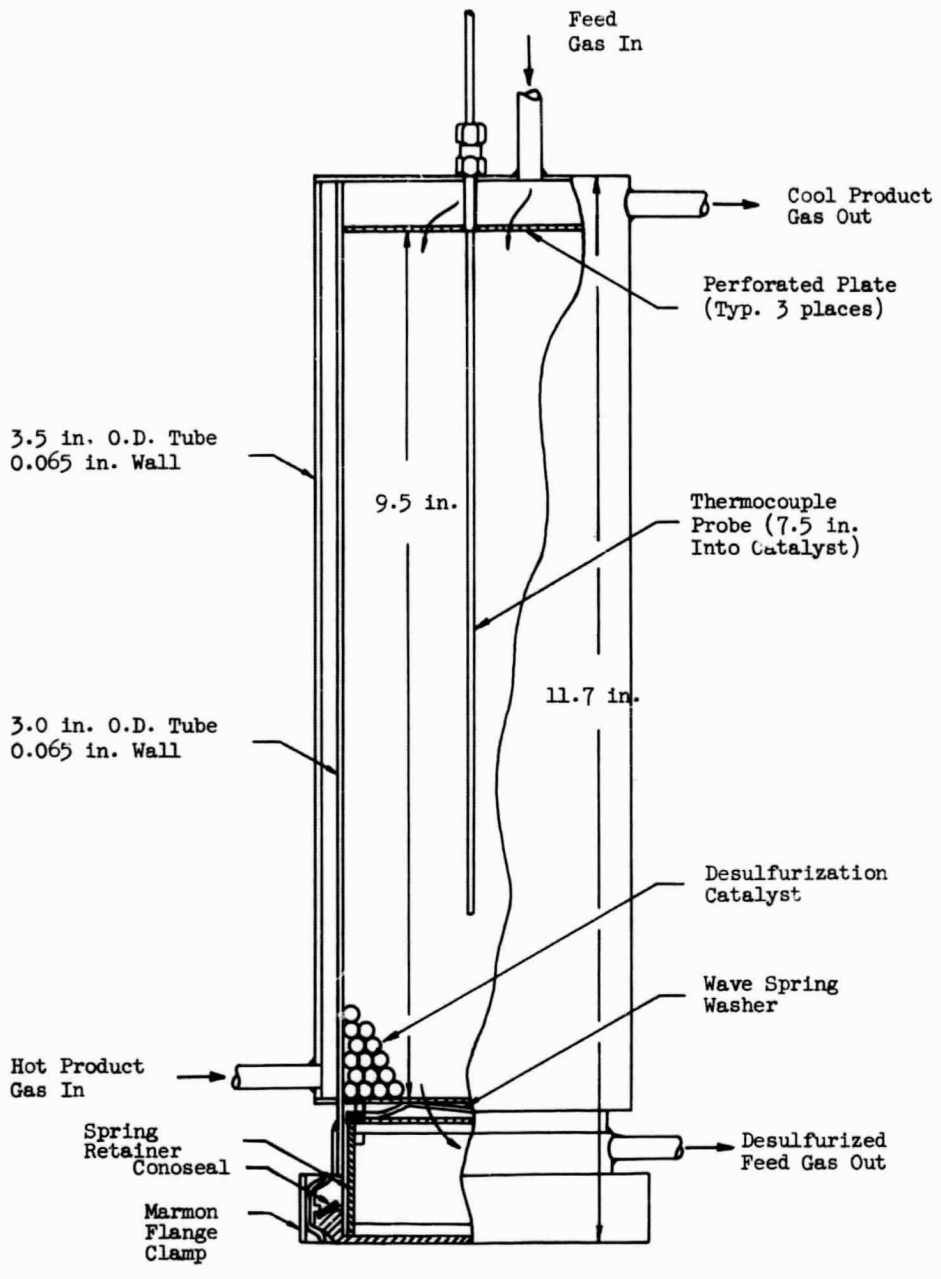

Figure 6.- Desulferization chamber schematic.

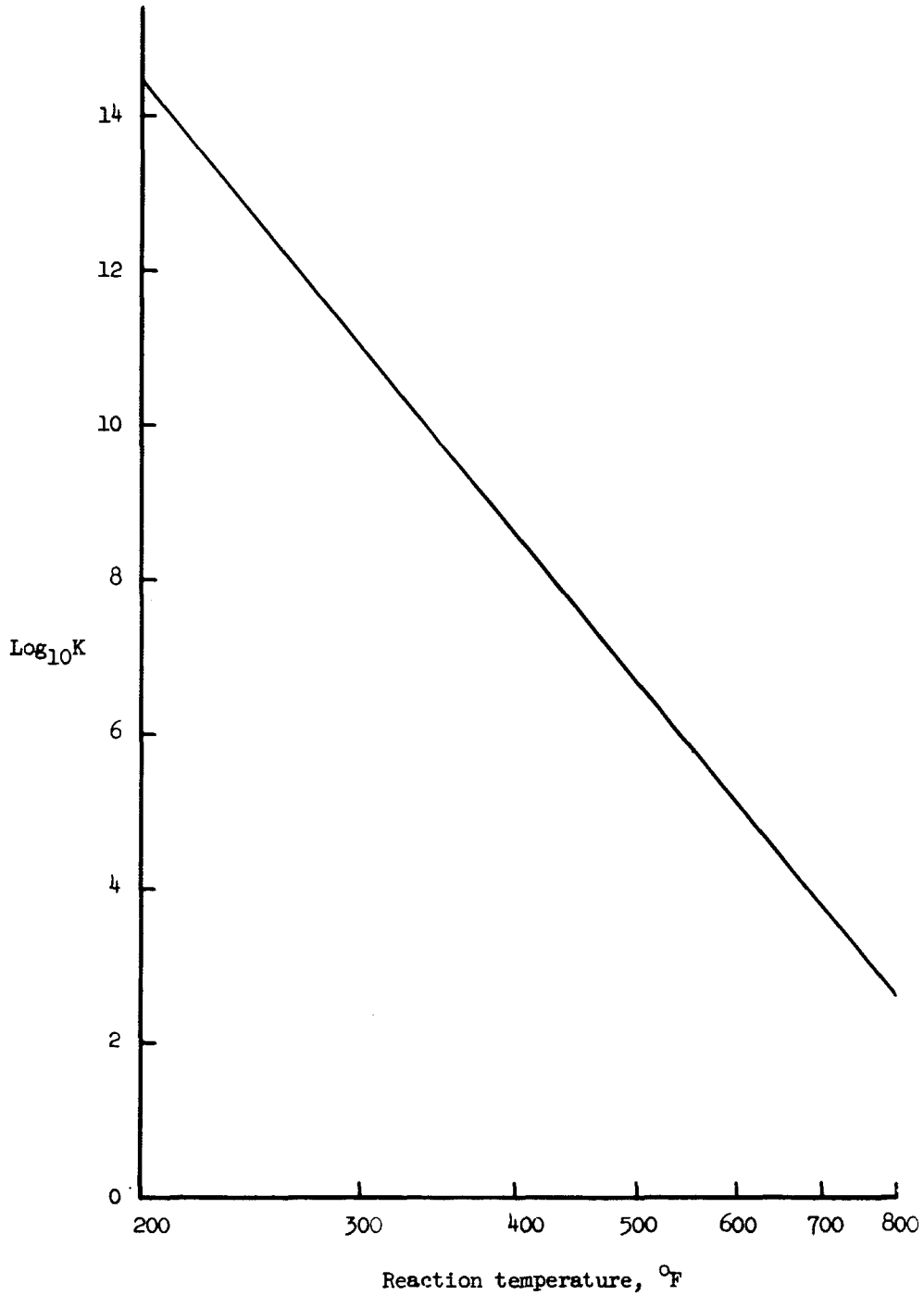

Figure 7.- Variation of equilibrium constant, K, with temperature.

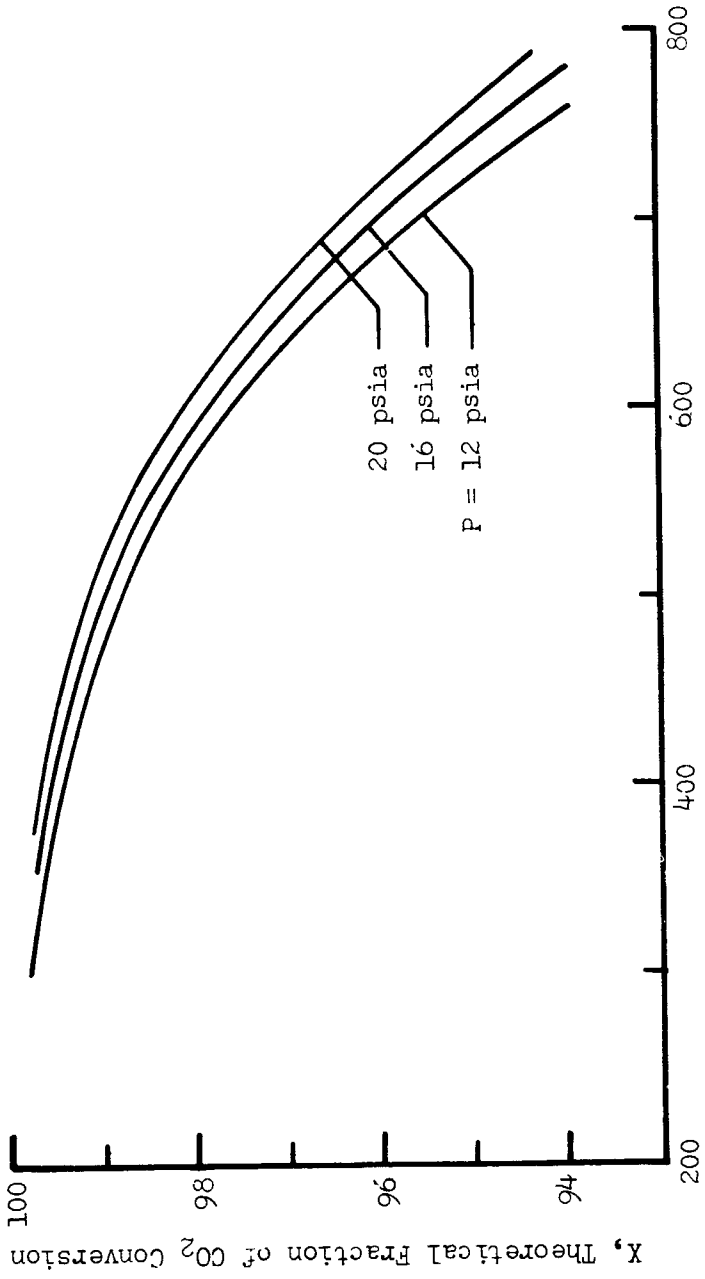

Figure 8.- Variation of the theoretical CO_2 equilibrium conversion with reaction temperature for constant reaction pressures and stoichiometric flow.

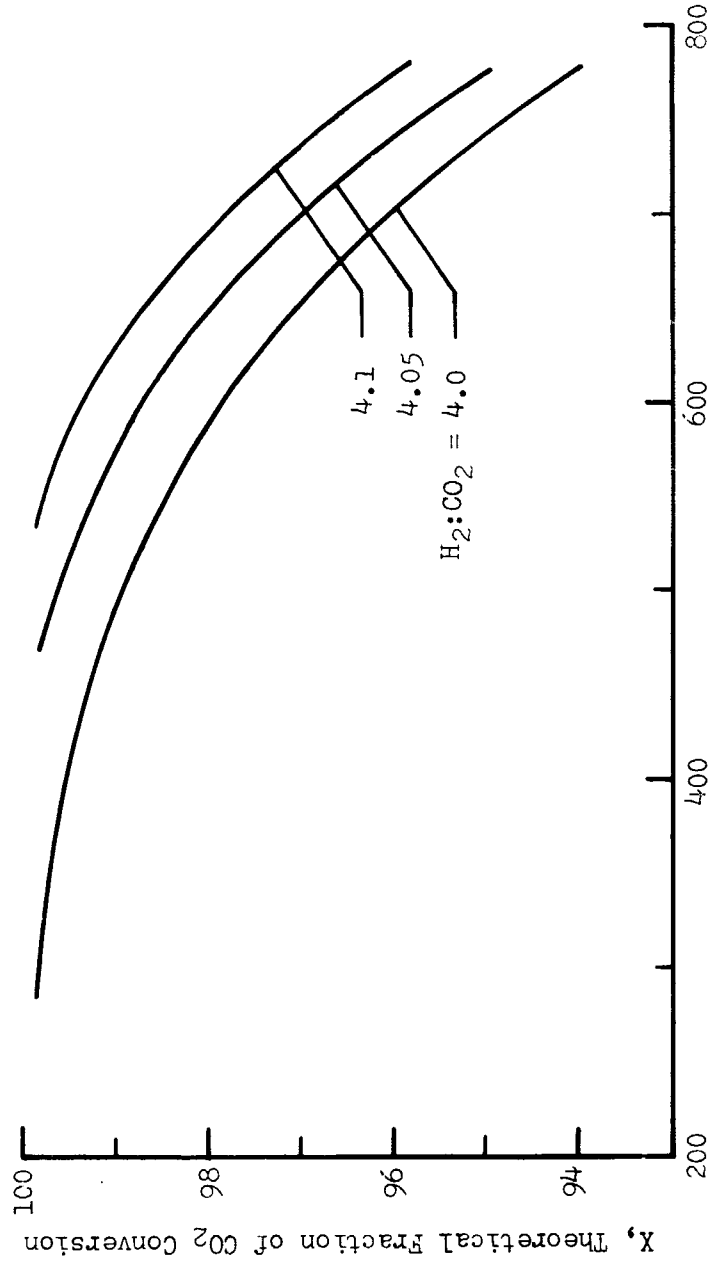

Figure 9.- Variation of the theoretical CO_2 equilibrium conversion with reaction temperature at 16 psia for constant $H_2:CO_2$ feed ratios.

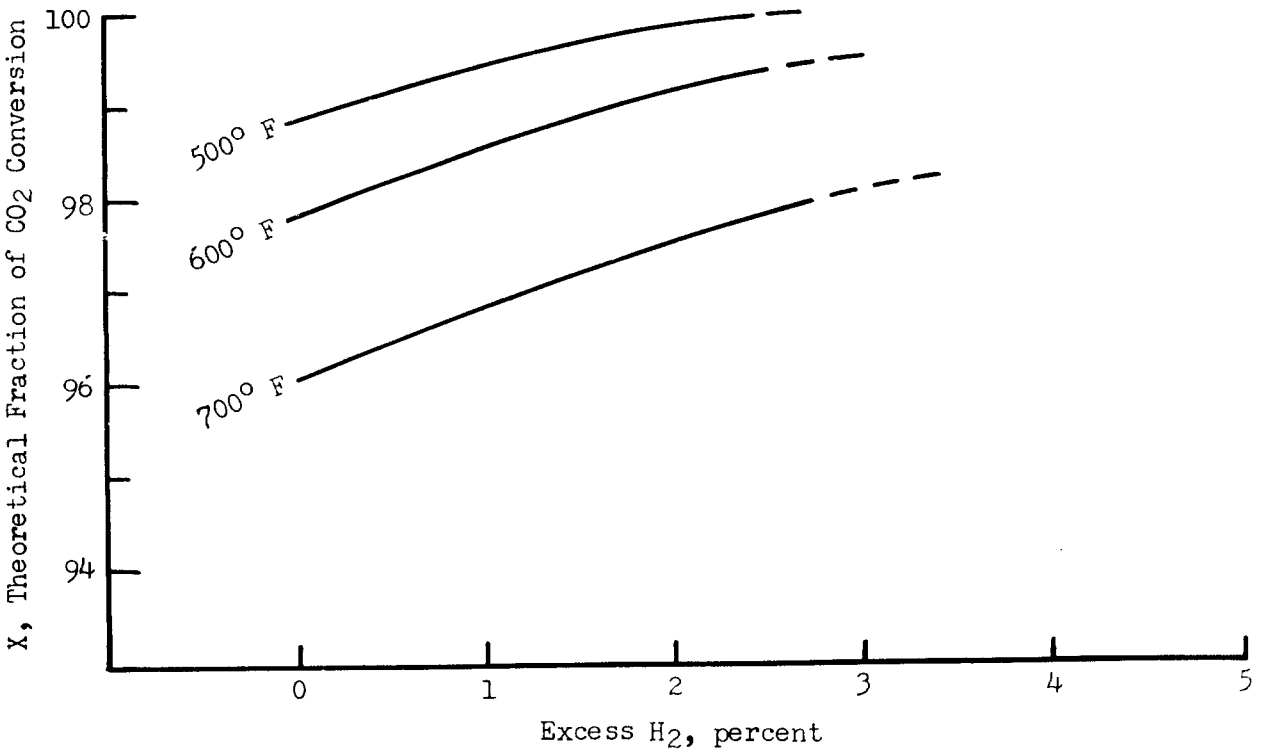

Figure 10.- Variation of the theoretical CO_2 equilibrium conversion with excess H_2 at 16 psia for constant reaction temperatures.

TABLE 1.- TABULATION OF DATA AND RESULTS FOR 16 PSIA

Run No.	$\dot{W}_{H_2}$, lb/day	Temp., °F	$H_2:CO_2$	Space velocity, hr^{-1}	$\dot{W}_{H_2O}$, lb/day	Outlet composition, percent volume				CO_2 conversion efficiency, percent
						CO_2	H_2	CH_4	H_2O	
5	0.5	450	4.00	174	1.96	5.0	14.5	77.2	3.7	93.5
37	1.0	300	4.38	342	3.66	1.0	30.0	67.5	2.9	87.8
11	1.0	400	3.72	354	3.91	12.0	3.7	80.6	4.0	85.8
13	1.0	400	4.75	338	3.36	1.3	28.7	67.3	3.0	97.7
14	1.0	400	4.26	344	3.50	5.5	13.8	76.7	2.7	91.9
15	1.0	400	5.25	334	3.08	0.0	48.6	48.8	2.7	100.0
16	1.0	400	3.44	360	3.60	14.9	3.2	77.8	2.6	80.0
17	1.0	400	3.18	367	3.68	21.0	1.1	73.4	2.6	73.6
12	1.0	450	5.02	335	3.50	0.0	37.0	61.2	3.8	100.0
10	1.0	500	4.00	349	4.48	4.4	16.6	76.4	3.8	95.3
18	1.0	500	4.81	336	4.19	0.0	38.3	59.7	2.7	100.0
20	1.0	500	4.49	341	4.53	0.7	28.3	68.6	2.7	99.3

TABLE 1.- Continued

Run No.	$\dot{W}_{H_2}$, lb/day	Temp., °F	$H_2:CO_2$	Space velocity, hr^{-1}	$\dot{W}_{H_2O}$, lb/day	Outlet composition, percent volume				CO_2 conversion efficiency, percent
						CO_2	H_2	CH_4	H_2O	
21	1.0	500	4.35	343	3.84	1.6	22.8	72.3	2.6	97.8
22	1.0	500	3.67	355	4.24	10.1	4.6	81.2	2.6	88.6
23	1.0	500	3.46	359	4.22	14.6	1.4	80.0	2.6	83.9
24	1.0	500	3.21	366	4.35	20.0	0.0	75.8	2.7	79.0
25	1.0	500	3.00	372	4.40	25.1	0.0	71.2	2.6	74.1
36	1.0	500	4.35	344	4.29	1.1	28.0	69.2	3.5	98.7
27	1.0	600	3.44	360	5.00	10.4	6.5	82.4	2.9	90.7
28	1.0	600	4.00	348	4.45	1.6	21.8	75.9	3.1	98.0
29	1.0	600	2.83	377	4.45	25.2	0.0	71.9	2.9	73.3
30	1.0	600	4.55	340	4.31	0.0	37.8	61.8	3.1	100.0
31	1.0	600	4.18	345	4.15	0.4	28.2	70.7	3.1	99.4
32	1.0	600	3.22	367	4.65	16.2	0.8	79.4	3.1	83.3

TABLE 1.- Continued

Run No.	$\dot{W}_{H_2}$, lb/day	Temp., °F	$H_2:CO_2$	Space velocity, hr^{-1}	$\dot{W}_{H_2O}$, lb/day	Outlet composition, percent volume				CO_2 conversion efficiency, percent
						CO_2	H_2	CH_4	H_2O	
34	1.0	600	4.32	344	4.51	1.7	20.6	75.7	3.8	98.3
35	1.0	600	3.05	369	4.45	22.3	2.4	73.1	3.9	80.2
9	1.25	500	4.00	437	5.06	4.0	14.8	77.7	3.7	94.9
4	1.5	500	4.00	523	6.10	5.5	13.0	80.2	3.5	93.4
76	1.5	500	5.10	500	5.52	0.0	46.6	48.9	3.0	100.0
77	1.5	500	4.39	510	5.94	0.0	35.0	62.0	3.0	100.0
78	1.5	500	4.32	516	6.25	1.3	27.0	69.8	3.0	98.3
79	1.5	500	4.00	523	6.36	4.5	16.5	77.3	3.0	94.6
80	1.5	500	3.90	526	6.79	6.2	13.0	78.8	3.0	93.7
81	1.5	500	3.67	533	6.57	9.7	8.3	80.0	2.9	89.5
82	1.5	500	3.42	541	6.69	14.5	6.5	78.0	3.1	85.0
83	1.5	500	3.18	550	7.27	19.2	4.5	74.8	3.3	82.2

TABLE 1.- Continued

Run No.	$\dot{W}_{H_2}$, lb/day	Temp., °F	$H_2:CO_2$	Space velocity, hr^{-1}	$\dot{W}_{H_2O}$, lb/day	Outlet composition, percent volume				CO_2 conversion efficiency, percent
						CO_2	H_2	CH_4	H_2O	
84	1.5	500	3.08	555	6.82	20.8	4.5	72.3	4.1	78.6
85	1.5	500	4.35	515	6.04	1.5	24.0	69.7	4.1	98.0
8	1.75	500	4.00	611	7.26	4.3	14.2	78.8	3.6	94.4
62	2.0	400	3.24	730	8.51	19.6	7.4	68.4	2.6	77.6
63	2.0	400	4.28	689	8.16	3.6	31.5	64.3	2.6	95.2
64	2.0	400	3.95	700	8.22	6.8	20.9	70.0	2.6	91.2
67	2.0	400	4.14	694	8.47	5.2	25.3	69.7	2.6	93.8
68	2.0	400	4.46	672	7.95	2.3	35.0	63.8	3.2	96.8
69	2.0	400	4.54	680	7.63	1.4	38.6	58.9	3.6	97.8
70	2.0	400	4.95	672	7.26	0.6	44.8	49.5	3.7	98.9
71	2.0	400	3.63	712	8.80	11.5	13.4	71.7	3.6	87.2
72	2.0	400	2.89	752	8.82	26.5	7.9	63.0	3.3	71.3

TABLE 1.- Continued

Run No.	$\dot{W}_{H_2}$, lb/day	Temp., °F	$H_2:CO_2$	Space velocity, hr^{-1}	$\dot{W}_{H_2O}$, lb/day	Outlet composition, percent volume				CO_2 conversion efficiency, percent
						CO_2	H_2	CH_4	H_2O	
3	2.0	500	4.13	694	8.16	3.4	18.0	77.8	3.4	95.8
7	2.0	500	4.00	700	8.30	6.4	10.5	79.8	4.0	92.6
41	2.0	500	4.10	695	8.32	3.2	21.5	74.6	2.7	95.9
42	2.0	500	4.23	690	8.05	2.2	23.2	72.7	2.7	97.1
43	2.0	500	4.30	687	8.27	1.4	26.3	70.2	2.8	98.2
44	2.0	500	4.47	683	8.06	0.6	32.8	64.8	2.9	99.1
45	2.0	500	4.65	679	9.11	0.0	36.5	62.0	2.9	100.0
46	2.0	500	4.17	680	8.90	6.4	13.2	77.3	2.9	95.0
48	2.0	500	3.29	736	9.57	22.0	3.7	70.4	2.8	79.5
49	2.0	500	3.44	720	9.12	17.6	4.8	72.3	2.5	82.6
50	2.0	500	3.75	707	8.75	10.1	9.6	77.1	2.5	89.2
73	2.0	500	2:89	751	9.09	26.3	6.4	66.0	3.2	72.9

TABLE 1.- Concluded

Run No.	$\dot{W}_{H_2}$, lb/day	Temp., °F	$H_2:CO_2$	Space velocity, hr^{-1}	$\dot{W}_{H_2O}$, lb/day	Outlet composition, percent volume				CO_2 conversion efficiency, percent
						CO_2	H_2	CH_4	H_2O	
74	2.0	500	3.44	720	8.88	15.5	8.4	73.4	3.1	83.6
75	2.0	500	3.98	699	8.53	5.4	14.8	76.0	3.0	93.5
54	2.0	600	4.13	694	9.00	2.6	17.3	77.3	2.5	97.2
55	2.0	600	4.33	688	8.70	1.3	35.2	62.8	2.4	98.3
56	2.0	600	4.44	684	8.53	0.5	27.5	70.1	2.4	99.4
57	2.0	600	3.76	706	8.54	7.6	7.9	81.2	2.5	91.3
58	2.0	600	2.70	765	9.81	32.9	2.0	62.4	2.5	69.8
59	2.0	600	3.54	715	9.83	13.2	4.2	77.4	2.6	88.6
60	2.0	600	2.91	750	9.62	28.1	3.0	65.8	2.5	73.8
61	2.0	600	3.26	730	9.28	19.2	3.0	73.4	2.7	81.2

TABLE 2.- TABULATION OF DATA AND RESULTS FOR 20 PSIA

Run No.	$\dot{W}_{H_2}$, lb/day	Temp., °F	$H_2:CO_2$	Space velocity, hr^{-1}	$\dot{W}_{H_2O}$, lb/day	Outlet composition, percent volume				CO_2 conversion efficiency, percent
						CO_2	H_2	CH_4	H_2O	
115	1.0	400	2.59	387	3.52	29.4	4.0	67.0	2.1	62.3
116	1.0	400	2.72	382	4.31	26.1	4.0	70.0	2.3	70.7
117	1.0	400	2.91	374	4.30	23.2	4.2	70.8	2.9	74.1
118	1.0	400	3.11	368	4.16	19.3	5.1	72.8	2.7	77.3
119	1.0	400	3.20	366	4.35	15.6	6.3	75.2	2.5	80.9
120	1.0	400	3.40	361	4.19	12.0	8.8	76.9	2.4	85.3
121	1.0	400	3.51	358	4.27	9.4	11.3	76.6	2.4	88.4
122	1.0	400	3.67	355	4.03	6.1	16.7	73.9	2.4	91.3
123	1.0	400	3.97	350	4.03	3.4	23.4	69.2	2.4	94.9
124	1.0	400	4.16	346	3.93	1.9	30.6	62.6	2.4	96.9
125	1.0	400	4.30	344	3.82	[illegible]	37.0	60.4	2.4	98.1
87	1.0	500	3.92	350	4.20	6.6	13.4	80.0	2.3	93.0

TABLE 2.- Continued

Run No.	$\dot{W}_{H_2}$, lb/day	Temp., °F	$H_2:CO_2$	Space velocity, hr^{-1}	$\dot{W}_{H_2O}$, lb/day	Outlet composition, percent volume				CO_2 conversion efficiency, percent
						CO_2	H_2	CH_4	H_2O	
88	1.0	500	2.95	373	4.19	27.0	1.7	70.4	2.3	71.2
92	1.0	500	4.87	336	3.31	0.0	48.2	49.4	2.0	100.0
93	1.0	500	4.23	344	3.52	1.2	29.8	67.8	2.0	97.8
94	1.0	500	4.56	340	3.63	0.0	41.2	56.6	2.0	100.0
95	1.0	500	3.94	352	4.45	3.9	19.5	78.6	2.0	95.5
98	1.0	500	3.54	353	4.24	8.2	11.2	81.7	2.4	90.0
99	1.0	500	2.91	376	4.61	24.4	2.4	74.3	2.4	75.7
102	1.0	600	2.84	378	5.19	25.5	2.0	72.2	1.4	77.7
104	1.0	600	3.15	367	4.77	17.2	2.5	79.8	2.0	83.5
106	1.0	600	2.86	376	4.45	26.0	2.0	70.8	2.3	72.8
107	1.0	600	4.71	338	3.99	0.0	45.3	52.6	2.1	100.0
108	1.0	600	4.16	346	4.14	0.0	25.4	72.2	2.1	100.0

TABLE 2.- Concluded

Run No.	$\dot{W}_{H_2}$, lb/day	Temp., °F	$H_2:CO_2$	Space velocity, hr^{-1}	$\dot{W}_{H_2O}$, lb/day	Outlet composition, percent volume				CO_2 conversion efficiency, percent
						CO_2	H_2	CH_4	H_2O	
109	1.0	600	3.54	358	4.50	7.2	8.5	83.2	2.1	91.8
110	1.0	600	3.35	362	4.50	12.5	4.5	82.5	2.1	86.6
111	1.0	600	3.16	367	4.88	15.8	4.2	80.6	2.1	84.9
113	1.0	600	2.85	377	4.77	22.8	2.2	74.5	2.1	77.1

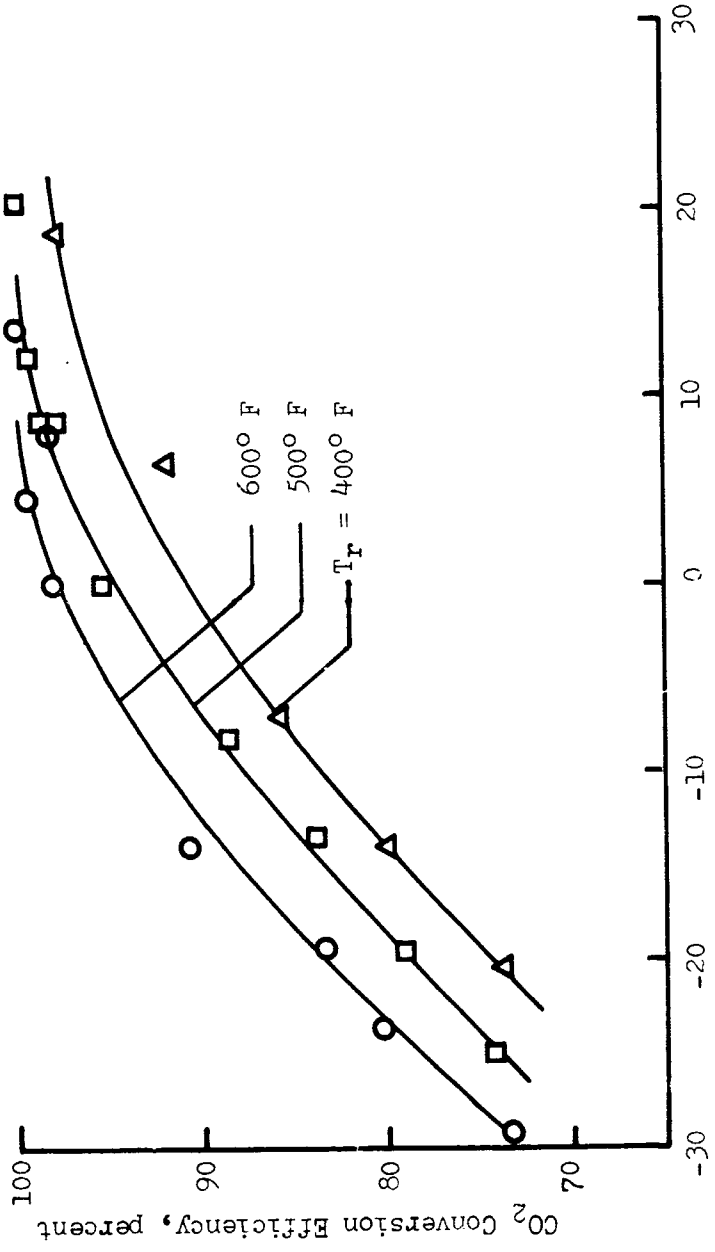

(a) $\dot{W}_{H_2} = 1.0 \frac{lb}{day}$

Figure 11.- Effect of excess H_2 on CO_2 conversion efficiency at 16 psia for constant reaction temperatures.

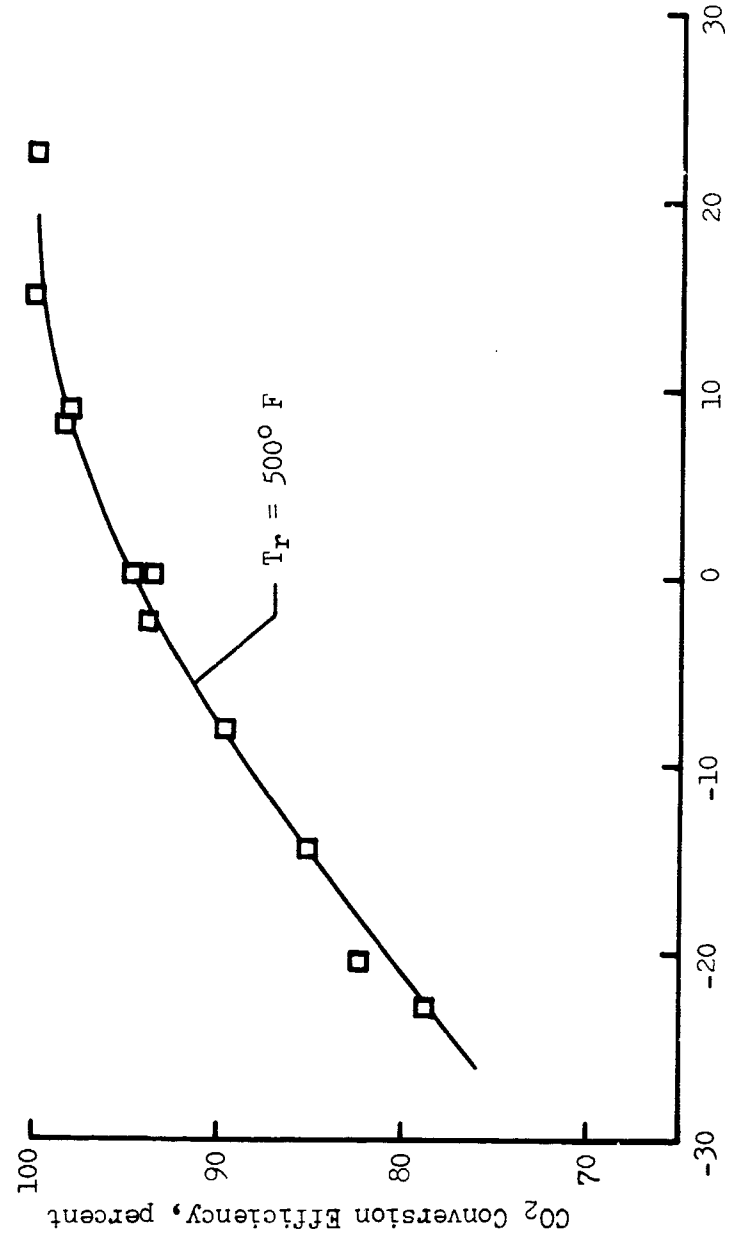

(b) $\dot{W}_{H_2} = 1.5 \frac{lb}{day}$

Figure 11.- Continued.

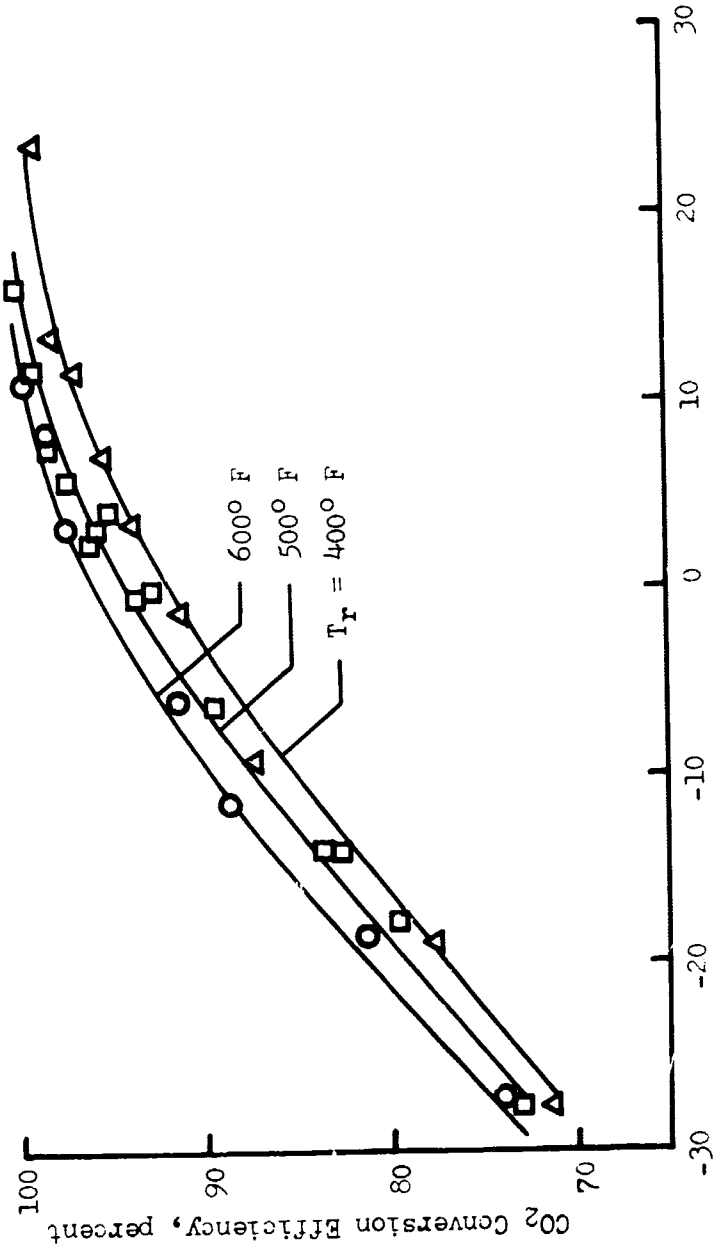

(c) $\dot{w}_{H_2} = 2.0 \frac{lb}{day}$

Figure 11.- Concluded.

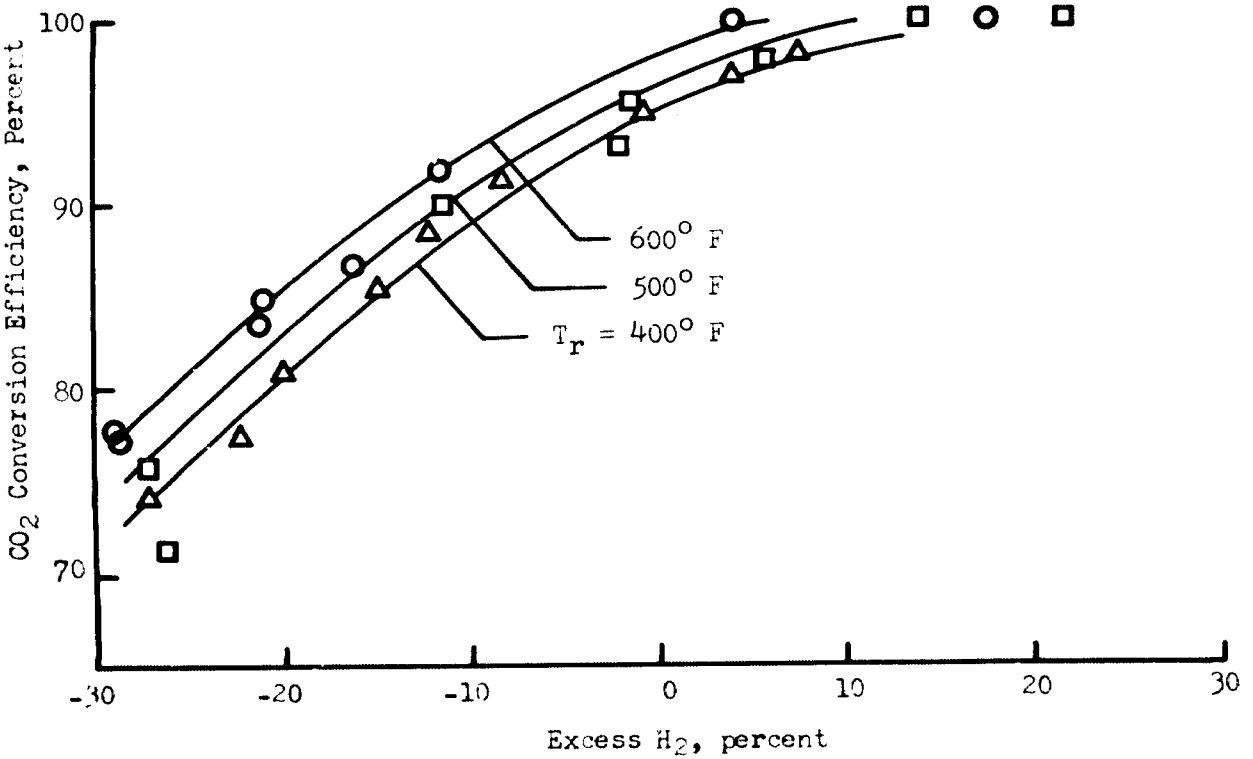

Figure 12.- Effect of excess H_2 on CO_2 conversion efficiency at 20 psia for constant reaction temperatures with $\dot{W}_{H_2} = 1.0 \frac{lb}{day}$.

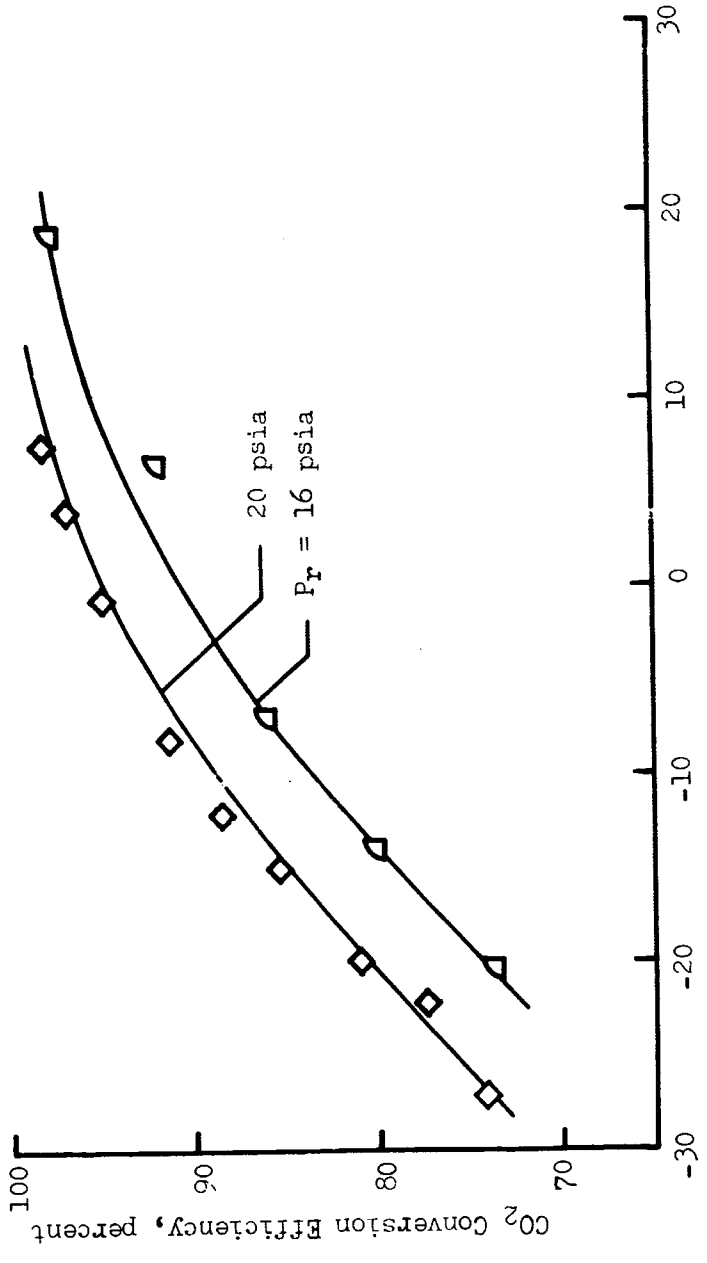

(a) T_r = 400° F

Figure 13.- Effect of excess H_2 on CO_2 conversion efficiency for constant reaction pressures with $\dot{W}_{H_2}$ = 1.0 $\frac{lb}{day}$.

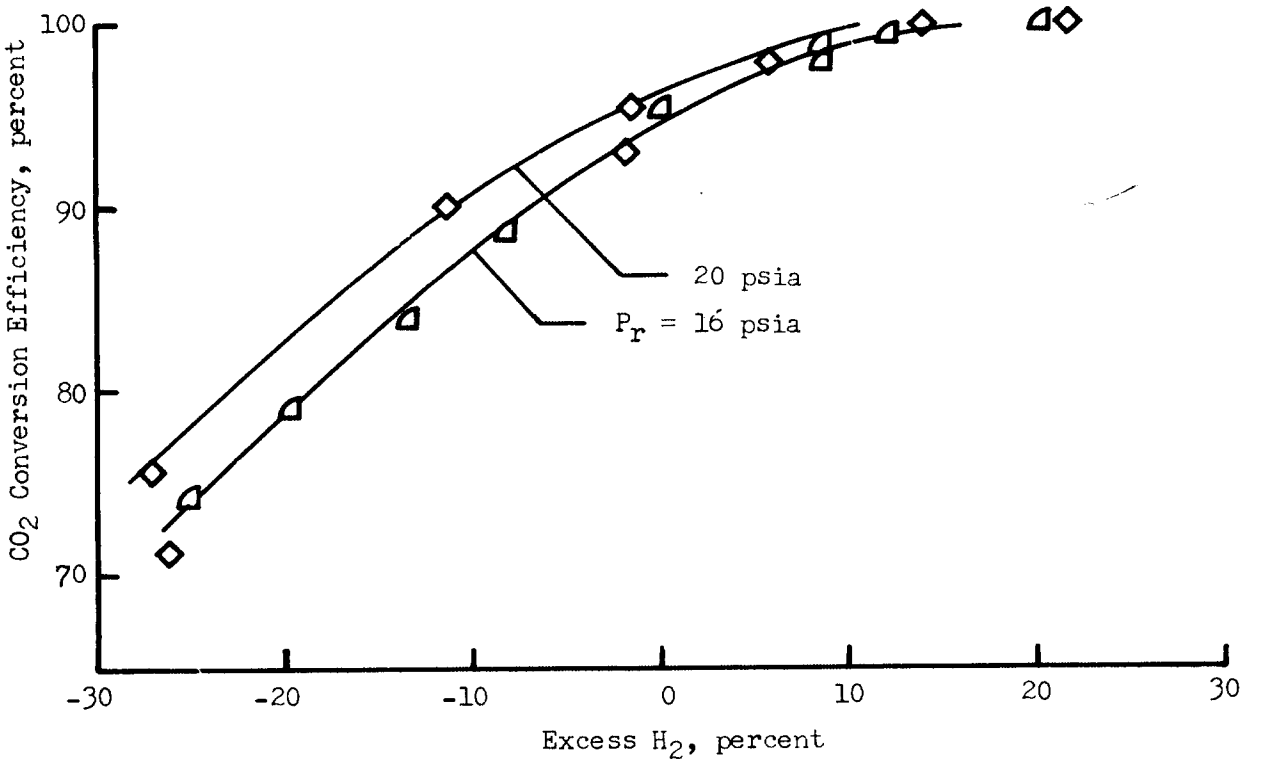

(b) $T_r = 500^o$ F

Figure 13.- Continued.

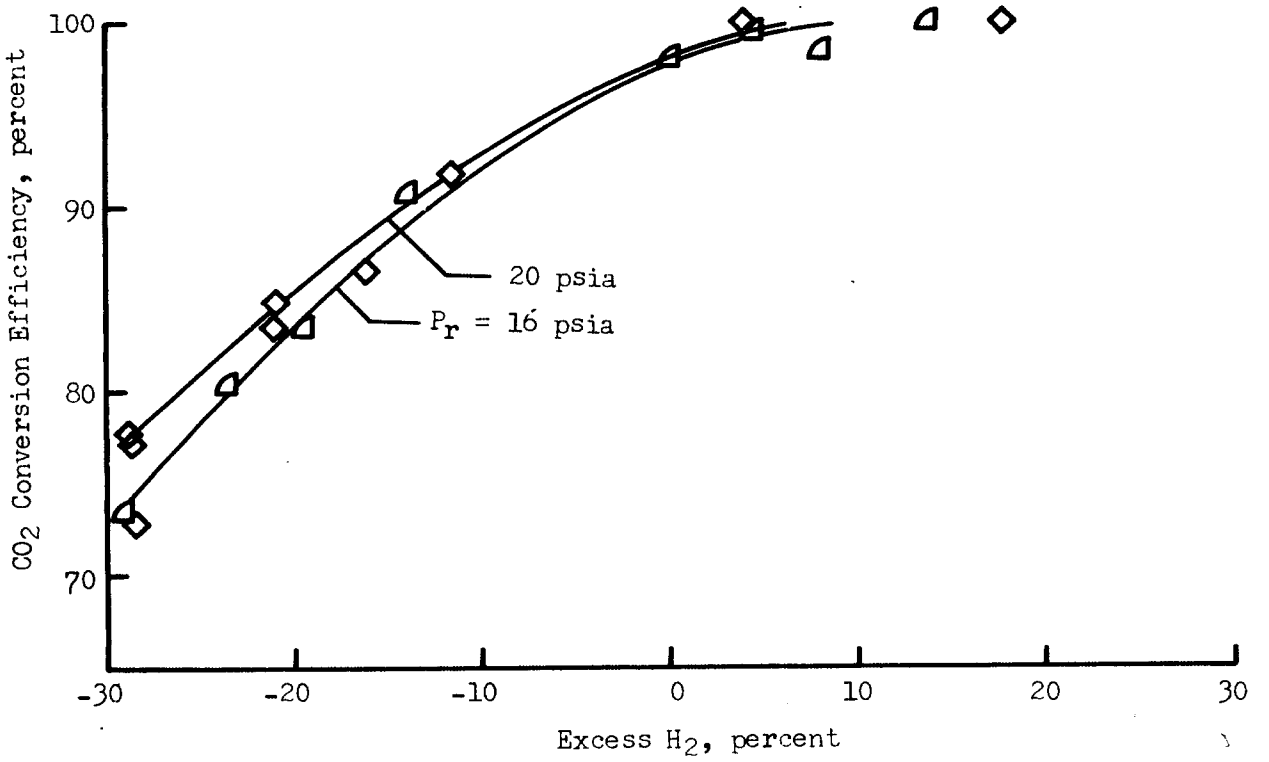

(c) $T_r = 600^\circ$ F

Figure 13.- Concluded.

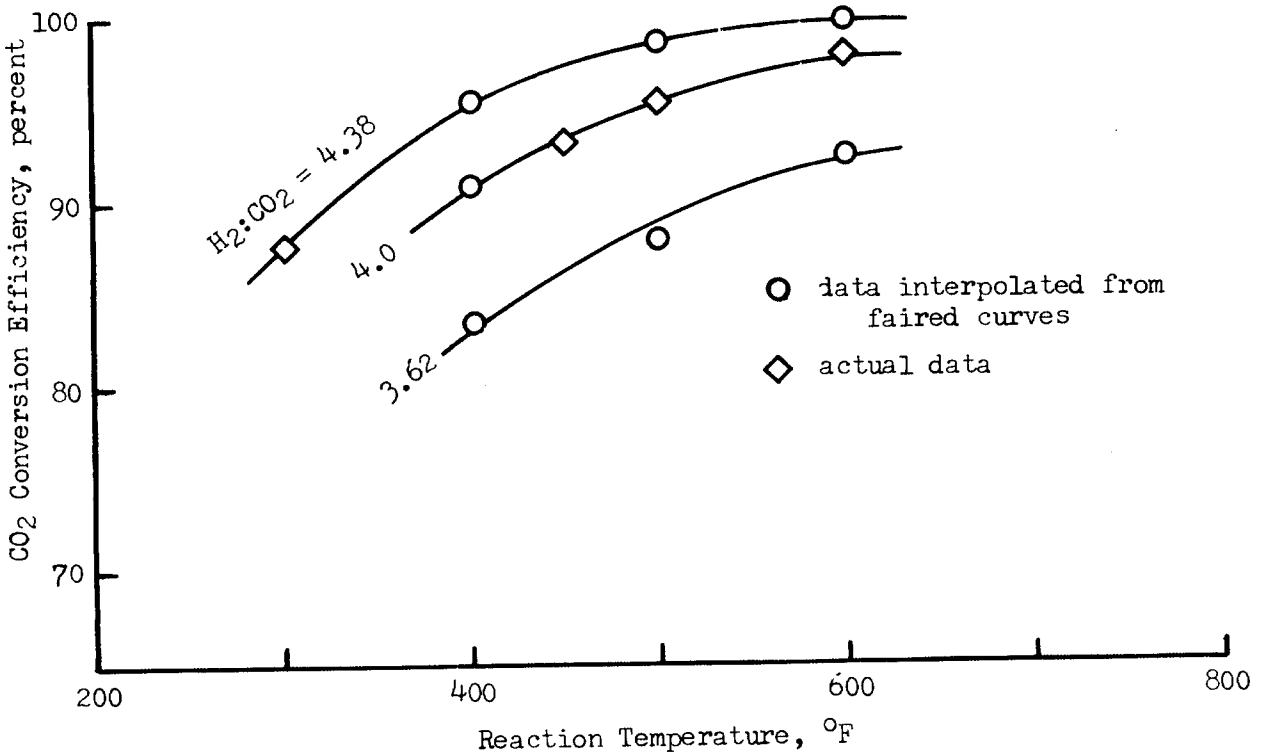

Figure 14.- Effect of reaction temperature on CO_2 conversion efficiency at 16 psia for constant $H_2:CO_2$ feed ratios with $\dot{W}_{H_2} = 1.0 \frac{lb}{day}$.

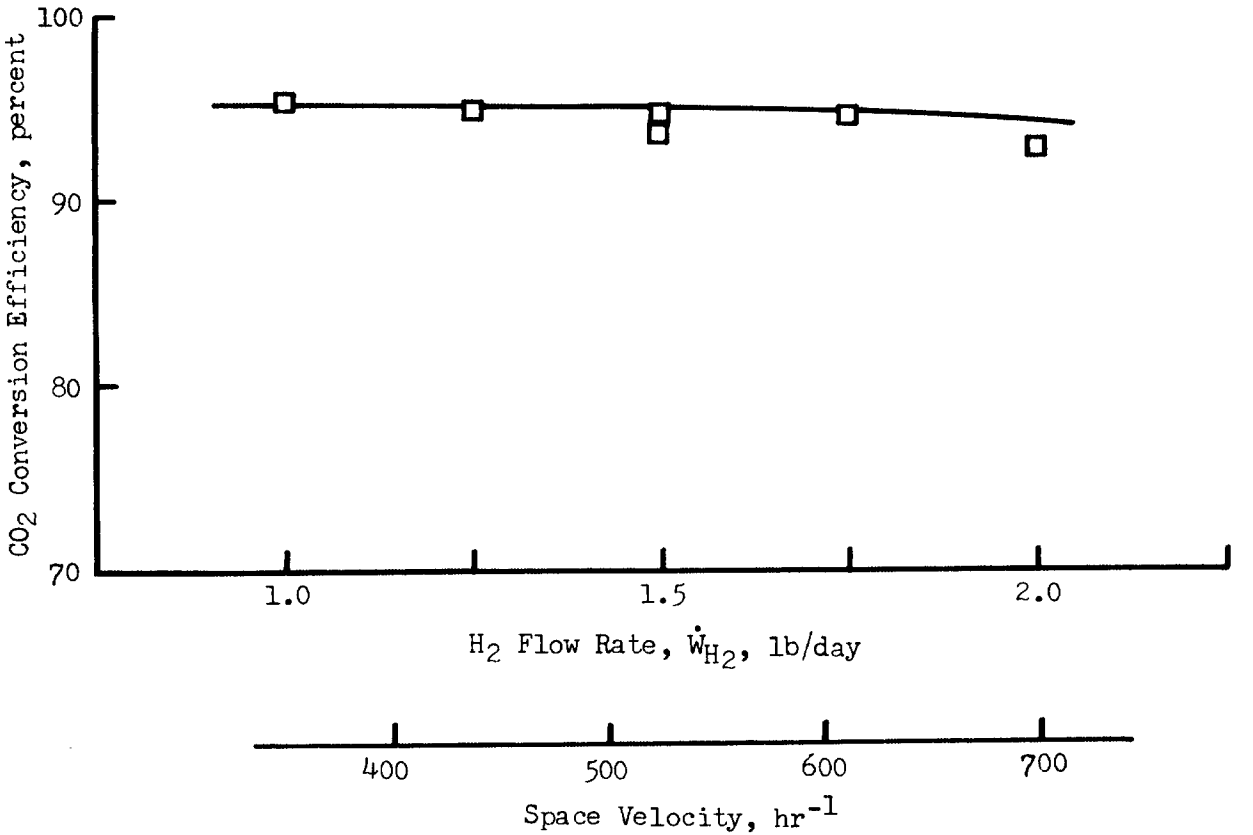

Figure 15.- Effect of flow rate on CO_2 conversion efficiency at 16 psia for stoichiometric at 16 psia flow with $T_r = 500^{\circ}$ F.

TABLE 3.- FREE-ENERGY FUNCTION, $\frac{(G_T^\circ - H_0^\circ)}{T}$, AND HEAT OF FORMATION, $\Delta H_{f_0}^\circ$, DATA

T, °K (°F)	Constituents			
	CO_2	H_2	CH_4	H_2O
	$\frac{(G_T^\circ - H_0^\circ)}{T}$, $\frac{\text{cal}}{(\text{g-mole } ^\circ\text{K})}$			
366 (200)	-45.071	-25.757	-38.061	-38.730
394 (250)	-45.694	-26.305	-38.719	-39.371
422 (300)	-46.232	-26.758	-39.276	-39.901
450 (350)	-46.746	-27.186	-39.805	-40.401
477 (400)	-47.251	-27.596	-40.305	-40.881
505 (450)	-47.742	-28.013	-40.832	-41.369
533 (500)	-48.183	-28.364	-41.291	-41.781
561 (550)	-48.624	-28.714	-41.750	-42.194
588 (600)	-49.061	-29.050	-42.178	-42.588
616 (650)	-49.462	-29.373	-42.625	-42.969
644 (700)	-49.853	-29.670	-43.037	-43.322
672 (750)	-50.243	-29.968	-43.448	-43.674
700 (800)	-50.634	-30.265	-43.860	-44.026
	$\Delta H_{f_0}^\circ$, $\frac{\text{cal}}{(\text{g-mole})}$			
-273 (0)	-93965	0	-15990	-57107

TABLE 4.- SABATIER REACTION EQUILIBRIUM CONSTANTS

T, ^{o}K (^{o}F)	Log_{10} K	K
366 (200)	14.518	3.296×10^{14}
394 (250)	12.789	6.151×10^{12}
422 (300)	11.296	1.976×10^{11}
450 (350)	9.975	9.440×10^{9}
477 (400)	8.829	6.745×10^{8}
505 (450)	7.766	5.834×10^{7}
533 (500)	6.819	6.591×10^{6}
561 (550)	5.956	9.036×10^{5}
588 (600)	5.185	1.531×10^{5}
616 (650)	4.466	2.924×10^{4}
644 (700)	3.806	6.397×10^{3}
672 (750)	3.192	1.556×10^{3}
700 (800)	2.620	4.093×10^{2}